

Dispersive properties of a magnetized degenerate electron gas

Jeanette I. Weise*

School of Physics, University of Sydney, NSW 2006, Australia

(Received 30 July 2008; published 31 October 2008)

Accurate dispersion relations are fundamental in the evaluation of many astrophysical processes such as, for example, heat loss by neutrino emission. In this paper, the parallel propagating wave modes of a magnetized, degenerate, electron gas are evaluated exactly using the S -matrix form of the linear response tensor (for a relativistic quantum magnetized electron gas) and the vertex formalism. The modes are then discussed in terms of the dissipative regions in which they occur. In addition to analogous modes to the unmagnetized case, there also exist doublet modes due to the logarithmic singularities that occur in the dissipative regimes of both the longitudinal and transverse dispersion relations and modes above the gyromagnetic thresholds for one of the transverse components. These additional modes only appear over a restricted range of wave numbers and are unique to the magnetized case.

DOI: [10.1103/PhysRevE.78.046408](https://doi.org/10.1103/PhysRevE.78.046408)

PACS number(s): 52.25.Mq, 12.20.-m, 52.27.Ny

I. INTRODUCTION

Although the dispersive properties for an unmagnetized degenerate electron gas have been extensively studied (see e.g., [1–6]), the same cannot be said for the dispersive properties of a magnetized degenerate electron gas. The prevalence of magnetic fields in most astrophysical environments justifies a more comprehensive study of the modes for a magnetized gas. Previous work in the magnetized regime consists of the following. Cover, Kalman and Bakshi [7] presented exact expressions for the real parts of the longitudinal and transverse dielectric response tensors in the limit $k_z=0$ for parallel propagating photons in a magnetized degenerate electron gas. Kowalenko, Frankel, and Hines [3] did likewise but only for the longitudinal mode and Landau quantum number $n=0$ along with its imaginary parts for arbitrary k_z . Pulsifer and Kalman [8] presented graphs of the longitudinal dispersion relations for parallel propagating photons in a magnetized degenerate gas in the pair creation regime emphasizing the existence of the pair modes—modes appearing above the pair creation thresholds above a critical wave number for both the longitudinal and transverse modes. They did not, however, give explicit forms for the real parts of the response tensors. Pérez Rojas and Shabad [9] discussed the forms of the dispersion relations near the two thresholds (pair creation and gyromagnetic absorption) and gave a comprehensive account of the absorption regions due to pair creation (above the pair creation threshold) and excitation of particles for the longitudinal mode (below the gyromagnetic absorption edge), in the degenerate limit in the $k_z, k_z^2 - \omega^2$ plane (parallel propagation).

In this paper, exact expressions for the Hermitian parts of the linear response tensors for a given magnetic field B and Fermi momentum p_F are presented, allowing for solutions to the dispersion relations. This was made possible by elect-

ing to consider a degenerate electron gas and parallel propagation ($\mathbf{k} \parallel \mathbf{B}$). For a degenerate electron gas, the temperature T of the electrons must satisfy $T \ll T_F$ where $T_F (=5.930 \times 10^9 \{[1 + (p_F/m)^2]^{1/2} - 1\} \text{ K})$ is the Fermi temperature and p_F is the Fermi momentum which is related to the cube root of the mass density of electrons. For a given Fermi momentum, this limits the temperature of the electrons for which the results derived here are valid.

Neutrino emission in the interior of very hot or dense stars is an effective heat loss mechanism. The rate of neutrino production is significantly affected by the presence of a background plasma which instigates the plasma process, the decay of plasmons and photons into neutrino pairs. As the degenerate, electron gases that exist in the interior of stars are magnetized, a thorough understanding of the wave modes of a magnetized, degenerate, electron gas is crucial if one is to study such heat loss mechanisms. Such a study is timely as there has been renewed interest in this field for unmagnetized plasmas (e.g., the neutrino luminosity of white dwarfs [10], energy losses in stars [11]). Analysis of the plasma process for a magnetized, degenerate, electron gas is underway and will be reported elsewhere.

The paper is set out as follows. In Sec. II, the polarization tensor for a degenerate electron gas is evaluated in the dissipative (above the pair creation threshold ω_{PC} and below the gyromagnetic absorption edge ω_{GA}) and nondissipative ($\omega_{GA} < \omega < \omega_{PC}$) regimes. In Sec. III, the dispersion relations are solved for photons propagating in the direction of the magnetic field (chosen to be in the z direction) such that the 4-wave vector of the photon is given by $k=(\omega, 0, 0, k_z)$. As well as solutions similar to those found for an unmagnetized degenerate electron gas, there also exist pair and gyromagnetic absorption modes in the dissipative regime $\omega > \omega_{PC}$ and $\omega < \omega_{GA}$, respectively as well as solutions near the gyromagnetic absorption edges for one of the transverse modes which are nonexistent for the unmagnetized case. In Sec. IV, the results are discussed and comparisons are made with the unmagnetized, degenerate limit and previous work.

*weise@physics.usyd.edu.au

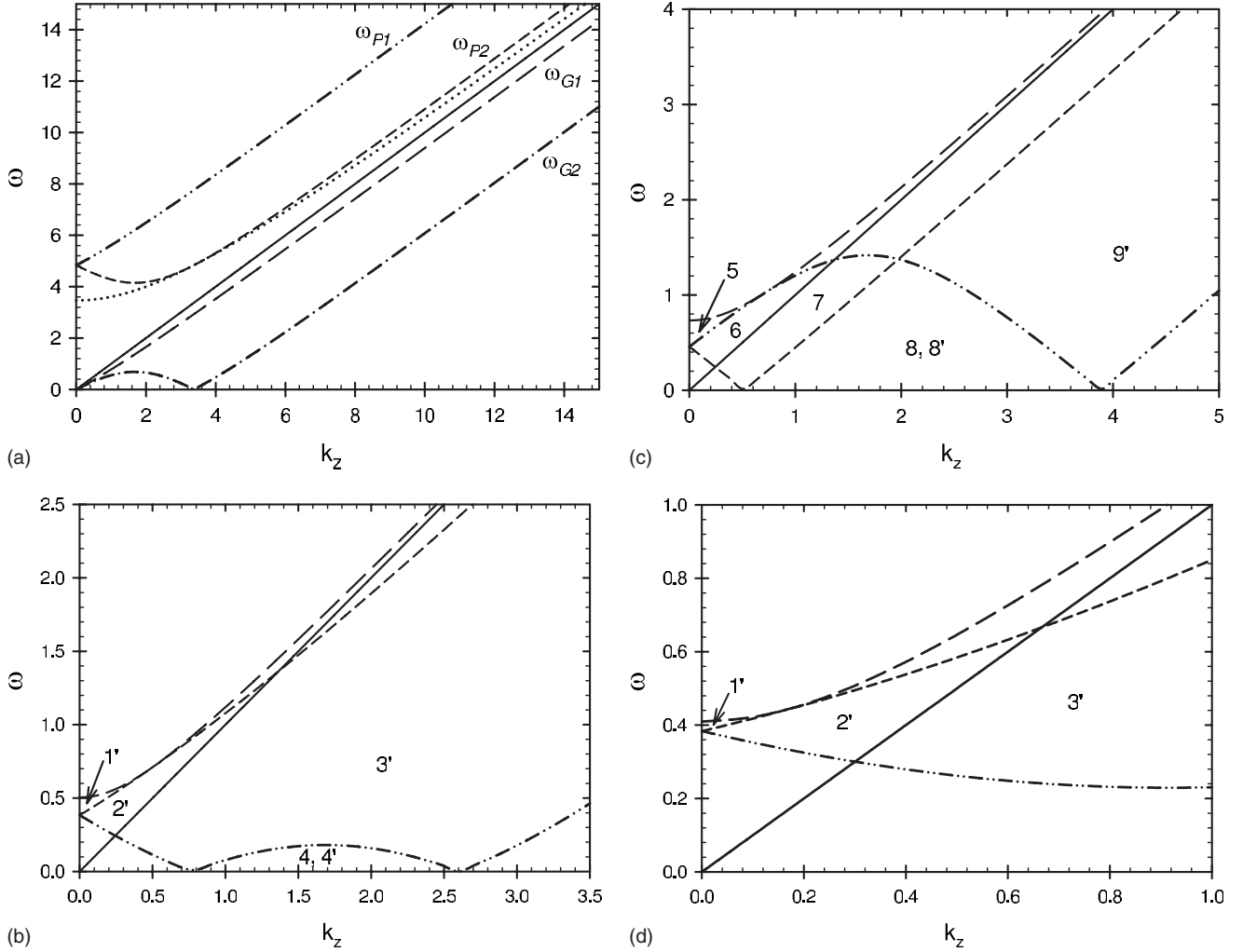


FIG. 1. (a): The boundaries of the different regions in the ω - k_z plane for α^{33} , parameters $p_F=2.2m$, $B=B_{cr}$, and $n=1$. The solid and dotted lines are the $\omega=k_z$ and $\omega=\omega_{PC|n=1}$ lines, respectively. The dashed-double-dotted and short-dashed lines, labeled ω_{P1} and ω_{P2} , are the $\omega=(\varepsilon_F^2 \pm 2p_1k_z + k_z^2)^{1/2} + \varepsilon_F$ lines, respectively. The long-dashed and dashed-dotted lines, labeled ω_{G1} and ω_{G2} , are the $\omega=|(\varepsilon_F^2 \pm 2p_1k_z + k_z^2)^{1/2} - \varepsilon_F|$ lines, respectively. (b) The boundaries of the different numbered regions in the GA dissipative regime of α^{11} and $i\alpha^{12}$, parameters $p_F=2.2m$, $B=B_{cr}$, and $\eta=1$ for I_A ($\eta=n$) and I_B ($\eta=n'$), polarizations e_{\pm}^{μ} , respectively. The solid and long-dashed lines are the $\omega=k_z$ and $\omega=\omega_{GA|n=1}$ lines, respectively. The short-dashed and dashed-double-dotted lines are the $\omega=|(\varepsilon_F^2 \pm 2p_1k_z + k_z^2 + 2eB)^{1/2} - \varepsilon_F|$ lines, respectively. (c) As for (b), but for I_D ($\eta=n$) and I_C ($\eta=n'$), polarizations e_{\pm}^{μ} , respectively, with the short-dashed and dashed-double-dotted lines here being the $\omega=|(\varepsilon_F^2 \pm 2p_1k_z + k_z^2 - 2eB)^{1/2} - \varepsilon_F|$ lines, respectively. (d) As for (b), but for $\eta=2$.

II. RESPONSE TENSORS

The general expression for the S -matrix form of the linear response tensor for a relativistic quantum magnetized electron gas is [12]

$$\alpha^{\mu\nu}(k) = -\frac{e^3 B}{2\pi} \sum_{\epsilon, q, \epsilon', q'} \int_{-\infty}^{\infty} \frac{dp_z}{2\pi} \int_{-\infty}^{\infty} \frac{dp'_z}{2\pi} 2\pi \delta(\epsilon' p'_z - \epsilon p_z + k_z) \frac{\epsilon n_q^{\epsilon}(p_z) - \epsilon' n_{q'}^{\epsilon'}(p'_z)}{\omega - \epsilon \varepsilon_q + \epsilon' \varepsilon_{q'} + i0} [\Pi_{q'q}^{\epsilon'\epsilon}]^{\mu\nu}, \quad (1)$$

where $[\Pi_{q'q}^{\epsilon'\epsilon}]^{\mu\nu}$ is the product of two vertex functions, viz.

$$[\Pi_{q'q}^{\epsilon'\epsilon}]^{\mu\nu} = [\Gamma_{q'q}^{\epsilon'\epsilon}(\mathbf{k})]^{\mu} [\Gamma_{q'q}^{\epsilon'\epsilon}(\mathbf{k})]^{*\nu}, \quad (2)$$

defined by (50) in Melrose and Parle [13]. The quantum numbers q, q' include the Landau quantum numbers n, n' , the spins σ, σ' , and the parallel (to the magnetic field) momenta p_z, p'_z . The contribution for given n, n' is related to one-photon pair creation with n, n' determining the incoming and outgoing energy eigenvalues (using natural units with $\hbar=c=1$), $\varepsilon_n(p_z) = (m^2 + p_z^2 + 2neB)^{1/2}$ and $\varepsilon_{n'}'(p'_z) = (m^2 + p_z'^2 + 2n'eB)^{1/2}$, respectively, of the electron and positron, with $k_z = \epsilon p_z - \epsilon' p'_z$ relating the components along \mathbf{B} of the 3-momenta of the photon, the electron ($\epsilon', \epsilon=+$) and the positron ($\epsilon', \epsilon=-$). Taking the degenerate limit of the plasma contribution for which the occupation numbers are unity for the electrons ($n_q^+ = n_{q'}^+ = 1$) with energies below the Fermi en-

ergy (zero otherwise) and zero for the positrons ($n_q^- = n_q^-, = 0$), and then summing over ϵ, ϵ' and the spins σ, σ' (where only the $[\Pi_{q'q}^{\epsilon'\epsilon}]^{\mu\nu}$ have spin dependences), one obtains

$$\alpha^{\mu\nu}(k) = -\frac{e^3 B}{2\pi} \sum_{n,n'}^{n_{\max}} \left[\int_{-p_n}^{p_n} \frac{dp_z}{2\pi} \left(\frac{[\Pi_{n'n}^+]^{\mu\nu}}{\omega - \epsilon + \epsilon' + i0} \right) \Big|_{p_z'=p_z-k_z} \right. \\ \left. + \frac{[\Pi_{n'n}^+]^{\mu\nu}}{\omega - \epsilon - \epsilon' + i0} \Big|_{p_z'=-p_z+k_z} \right) \\ - \int_{-p_{n'}}^{p_{n'}} \frac{dp_z'}{2\pi} \left(\frac{[\Pi_{n'n'}^+]^{\mu\nu}}{\omega - \epsilon + \epsilon' + i0} \right) \Big|_{p_z=p_z'+k_z} \\ \left. + \frac{[\Pi_{n'n'}^+]^{\mu\nu}}{\omega + \epsilon + \epsilon' + i0} \Big|_{p_z=-(p_z'+k_z)} \right), \quad (3)$$

with $p_n = (p_F^2 - 2n_e B)^{1/2}$, $p_{n'} = (p_F^2 - 2n' e B)^{1/2}$ both real such that if $2n_{\max} e B < p_F^2 \leq 2(n_{\max} + 1) e B$ then the sums over n', n extend from $n', n=0$ to $n', n=n_{\max}$, and $[\Pi_{n'n}^{\epsilon'\epsilon}]^{\mu\nu} = \Sigma_{\sigma, \sigma'} [\Gamma_{q'q}^{\epsilon'\epsilon}(\mathbf{k})]^\mu [\Gamma_{q'q}^{\epsilon'\epsilon}(\mathbf{k})]^{*\nu}$, the values of which are given

in the Appendix for $\mathbf{B}=(0,0,B)$ and $\mathbf{k}=(k_\perp \cos \psi, k_\perp \sin \psi, k_z)$.

With the restriction $\mathbf{k} \parallel \mathbf{B}$ ($k_\perp=0$), so that $k=(\omega, 0, 0, k_z)$, the J -functions, which appear in $[\Pi_{n'n}^{\epsilon'\epsilon}]^{\mu\nu}$ and are related to the Laguerre polynomials, are greatly simplified such that $J_{n'-n}^n$ and $J_{n'-n}^{n-1}$ are only nonzero when $n'=n$ with $n \geq 0$ and $n \geq 1$, respectively, having values of unity, and $J_{n'-n+1}^{n-1}$ and $J_{n'-n-1}^n$ are only nonzero (unity) when $n'=n-1$ ($n > 0$) and $n'=n+1$ ($n \geq 0$), respectively. Hence the only components of the linear response tensor that are nonzero are $\alpha^{00}, \alpha^{03}, \alpha^{30}, \alpha^{33}$ with $n'=n$ and $\alpha^{11} = \alpha^{22}, \alpha^{12} = -\alpha^{21}$ with $n'=n \pm 1$. Further, as $\alpha^{00}, \alpha^{03}, \alpha^{30}$ are expressible in terms of α^{33} say, viz.

$$\alpha^{03} = \alpha^{30} = \frac{k_z \alpha^{33}}{\omega}, \quad \alpha^{00} = \frac{k_z^2 \alpha^{33}}{\omega^2},$$

via the charge continuity and gauge invariant relations, one need only evaluate α^{33} explicitly.

Substituting in the forms of $[\Pi_{n'n}^{\epsilon'\epsilon}]^{\mu\nu}$ and after some rearrangement, the $\alpha^{33}, \alpha^{11}, i\alpha^{12}$ components, in the dissipative regimes above the pair creation threshold and below the gyromagnetic absorption edge, are of the form

$$\alpha^{33} = \frac{e^3 B}{2\pi} \sum_{n=0}^{n_{\max}} \frac{\epsilon_n^{02} \omega^2 a_n}{2\pi(\omega^2 - k_z^2)^2} \int_{-p_n}^{p_n} \frac{dp_z}{\epsilon_n} \left(\frac{(\omega^2 - k_z^2) + 2k_z p_z + 2\omega \epsilon_n}{(p_z - \alpha_0 - \beta_0 - i0)(p_z - \alpha_0 + \beta_0 + i0)} + \frac{(\omega^2 - k_z^2) - 2k_z p_z - 2\omega \epsilon_n}{(p_z + \alpha_0 - \beta_0 - i0)(p_z + \alpha_0 + \beta_0 + i0)} \right), \\ \alpha^{11} = \frac{e^3 B}{16\pi^2(\omega^2 - k_z^2)} (A + C + D + B), \\ i\alpha^{12} = \frac{e^3 B}{16\pi^2(\omega^2 - k_z^2)} (-A + C - D + B), \\ A = \sum_{n=0}^{n_{\max}} \int_{-p_n}^{p_n} \frac{dp_z}{2\epsilon_n} \left(4(\omega^2 - k_z^2) + \frac{[\omega^2 - k_z^2 - 2(2n+1)eB](\omega^2 - k_z^2 - 2eB + 2p_z k_z + 2\omega \epsilon_n)}{(p_z - \alpha_1 - \beta_1 - i0)(p_z - \alpha_1 + \beta_1 + i0)} \right), \\ C = \sum_{n=1}^{n_{\max}} \int_{-p_n}^{p_n} \frac{dp_z}{2\epsilon_n} \left(4(\omega^2 - k_z^2) + \frac{[\omega^2 - k_z^2 - 2(2n-1)eB](\omega^2 - k_z^2 + 2eB + 2p_z k_z + 2\omega \epsilon_n)}{(p_z - \alpha_2 - \beta_2 - i0)(p_z - \alpha_2 + \beta_2 + i0)} \right), \\ D = \sum_{n'=1}^{n_{\max}} \int_{-p_{n'}}^{p_{n'}} \frac{dp_z'}{2\epsilon_{n'}} \left(4(\omega^2 - k_z^2) + \frac{[\omega^2 - k_z^2 - 2(2n'-1)eB](\omega^2 - k_z^2 + 2eB - 2p_z' k_z - 2\omega \epsilon_{n'})}{(p_z' + \alpha_2 - \beta_2' - i0)(p_z' + \alpha_2 + \beta_2' + i0)} \right), \\ B = \sum_{n'=0}^{n_{\max}} \int_{-p_{n'}}^{p_{n'}} \frac{dp_z'}{2\epsilon_{n'}} \left(4(\omega^2 - k_z^2) + \frac{[\omega^2 - k_z^2 - 2(2n'+1)eB](\omega^2 - k_z^2 - 2eB - 2p_z' k_z - 2\omega \epsilon_{n'})}{(p_z' + \alpha_1 - \beta_1' - i0)(p_z' + \alpha_1 + \beta_1' + i0)} \right), \quad (4)$$

where

$$\alpha_0 = \frac{k_z}{2}, \quad \alpha_1 = \frac{k_z}{2} \left(1 - \frac{2eB}{\omega^2 - k_z^2} \right), \quad \alpha_2 = \frac{k_z}{2} \left(1 + \frac{2eB}{\omega^2 - k_z^2} \right),$$

$$\beta_0 = \frac{\omega}{2} \sqrt{1 - \frac{4\varepsilon_n^{02}}{\omega^2 - k_z^2}},$$

$$\beta_1 = \frac{\omega}{2} \sqrt{\frac{(\omega^2 - k_z^2 - 2eB)^2}{(\omega^2 - k_z^2)^2} - \frac{4\varepsilon_n^{02}}{\omega^2 - k_z^2}},$$

$$\beta_2 = \frac{\omega}{2} \sqrt{\frac{(\omega^2 - k_z^2 + 2eB)^2}{(\omega^2 - k_z^2)^2} - \frac{4\varepsilon_n^{02}}{\omega^2 - k_z^2}},$$

with $\varepsilon_n^{02} = m^2 + 2neB$ and a_n one-half for $n=0$ and unity for $n>0$. The thresholds for pair creation (PC) and gyromagnetic absorption (GA) result from the conditions $\beta_0, \beta_1, \beta_2 = 0$ and are given by $\omega_{PC} = (4\varepsilon_n^{02} + k_z^2)^{1/2}$, $[(\varepsilon_n^0 + \varepsilon_{n\pm 1}^0)^2 + k_z^2]^{1/2}$ and $\omega_{GA} = k_z$, $[(\varepsilon_n^0 - \varepsilon_{n\pm 1}^0)^2 + k_z^2]^{1/2}$, respectively. The values of β'_1, β'_2 and the relevant thresholds from the conditions $\beta'_1, \beta'_2 = 0$ are as for β_1, β_2 but with n replaced by n' . Note that the GA edge for α^{33} is at the light line, whereas for α^{11} and $i\alpha^{12}$, it lies above the light line. The upper signs on the $i0$ terms in the denominators are applicable for ω satisfying $0 < \omega < \omega_{PC}$ and $\omega > \omega_{PC}$ and the lower signs for ω satisfying $k_z < \omega < \omega_{GA}$. The first ($n \geq 0$, $n' = n+1$) and third ($n' \geq 1$, $n = n' - 1$) terms of $\alpha^{11}, i\alpha^{12}$ [A and D in (4)] are associated with left circular (LC) polarized photons, polarization $e_-^\mu = 2^{-1/2}(0, 1, -i, 0)$, and give rise to the imaginary components

labeled A and D, respectively, in (7). The second ($n' \geq 1$, $n = n' - 1$) and fourth ($n' \geq 0$, $n = n' + 1$) terms (C and B in (4)) are associated with right circular (RC) polarized photons, polarization $e_+^\mu = 2^{-1/2}(0, 1, +i, 0)$, and give rise to the imaginary components labeled C and B, respectively, in (7).

The integrals over p_z in (4) have poles at $p_z = (\alpha_i \pm \beta_i)$ and $-(\alpha_i \pm \beta_i)$ ($i=0, 1, 2$) when $-p_n < \alpha_i \pm \beta_i < p_n$ and $-p_n < -(\alpha_i \pm \beta_i) < p_n$, respectively. The real and imaginary parts of $\alpha^{33}, \alpha^{11}, i\alpha^{12}$ can be found using Plemelj's formula,

$$\frac{1}{f(p_z) \pm i0} = \mathcal{P} \left(\frac{1}{f(p_z)} \right) \mp i\pi \delta(f(p_z)), \quad (5)$$

where $f(p_z) = p_z - (\alpha_i \pm \beta_i)$, $p_z + (\alpha_i \pm \beta_i)$, \mathcal{P} denotes the Cauchy principal value of the integral (the real part) and the second term is the semiresidue, such that

$$\mp i\pi \int_{-p}^p dp_z g(p_z) \delta(f(p_z)) = \mp i\pi \sum_j \frac{g(p_{zj})}{|f'(p_{zj})|},$$

where the sum is over all the zeroes $f(p_{zj}) = 0$. With the integrals over p'_z treated in the same manner and using the notation

$$\alpha^{\mu\nu} = \sum_{\eta}^{\eta_{\max}} \alpha^{\mu\nu}|_{\eta}, \quad \eta = n, n', \quad (6)$$

the real and imaginary parts in the dissipative regimes ($0 < \omega < \omega_{GA}|_{\eta}$, $\omega > \omega_{PC}|_{\eta}$) are as follows:

$$\text{Re } \alpha^{33}|_{n'=n} = \frac{e^3 B}{2\pi^2} \frac{\varepsilon_n^{02} \omega^2 k_z a_n}{\varepsilon_k (\omega^2 - k_z^2)^2} \ln \left| \frac{4k_z^4 \varepsilon_n^{04} - (\omega^2 - k_z^2)^2 (p_n k_z - 2\varepsilon_k \varepsilon_F)^2}{4k_z^4 \varepsilon_n^{04} - (\omega^2 - k_z^2)^2 (p_n k_z + 2\varepsilon_k \varepsilon_F)^2} \right|,$$

$$\text{Im } \alpha^{33}|_{n'=n} = \frac{e^3 B}{2\pi} \frac{\varepsilon_n^{02} \omega^2 k_z a_n}{\varepsilon_k (\omega^2 - k_z^2)^2} I_0,$$

$$\text{Re } \alpha^{11}|_{\eta=n, n'} = \frac{e^3 B}{16\pi^2 (\omega^2 - k_z^2)} (A + C + D + B),$$

$$\text{Re } i\alpha^{12}|_{\eta=n, n'} = \frac{e^3 B}{16\pi^2 (\omega^2 - k_z^2)} (-A + C - D + B),$$

$$A = \left[2(\omega^2 - k_z^2) \ln \left(\frac{\varepsilon_F + p_n}{\varepsilon_F - p_n} \right) + \frac{[\omega^2 - k_z^2 - 2(2n+1)eB]k_z}{2\varepsilon_{k1}} \left(\ln \left| \frac{k_z^4 (\omega^2 - k_z^2 - 2eB)^2 - 4(\omega^2 - k_z^2)^2 (p_n k_z - \omega \varepsilon_{k1})^2}{k_z^4 (\omega^2 - k_z^2 - 2eB)^2 - 4(\omega^2 - k_z^2)^2 (p_n k_z + \omega \varepsilon_{k1})^2} \right| \right. \right. \\ \left. \left. + \ln \left| \frac{4k_z^4 \varepsilon_n^{04} - [p_n k_z (\omega^2 - k_z^2 - 2eB) - 2\varepsilon_{k1} \varepsilon_F (\omega^2 - k_z^2)]^2}{4k_z^4 \varepsilon_n^{04} - [p_n k_z (\omega^2 - k_z^2 - 2eB) + 2\varepsilon_{k1} \varepsilon_F (\omega^2 - k_z^2)]^2} \right| \right) \right] \Big|_{n \geq 0},$$

$$C = \left[2(\omega^2 - k_z^2) \ln \left(\frac{\varepsilon_F + p_n}{\varepsilon_F - p_n} \right) + \frac{[\omega^2 - k_z^2 - 2(2n-1)eB]k_z}{2\varepsilon_{k2}} \left(\ln \left| \frac{k_z^4 (\omega^2 - k_z^2 + 2eB)^2 - 4(\omega^2 - k_z^2)^2 (p_n k_z - \omega \varepsilon_{k2})^2}{k_z^4 (\omega^2 - k_z^2 + 2eB)^2 - 4(\omega^2 - k_z^2)^2 (p_n k_z + \omega \varepsilon_{k2})^2} \right| \right. \right. \\ \left. \left. + \ln \left| \frac{4k_z^4 \varepsilon_n^{04} - [p_n k_z (\omega^2 - k_z^2 + 2eB) - 2\varepsilon_{k2} \varepsilon_F (\omega^2 - k_z^2)]^2}{4k_z^4 \varepsilon_n^{04} - [p_n k_z (\omega^2 - k_z^2 + 2eB) + 2\varepsilon_{k2} \varepsilon_F (\omega^2 - k_z^2)]^2} \right| \right) \right] \Big|_{n \geq 1}$$

$$\begin{aligned}
D &= \left[2(\omega^2 - k_z^2) \ln \left(\frac{\varepsilon_F + p_{n'}}{\varepsilon_F - p_{n'}} \right) + \frac{(\omega^2 - k_z^2 - 2(2n' - 1)eB)k_z}{2\varepsilon'_{k2}} \left(-\ln \left| \frac{k_z^4(\omega^2 - k_z^2 + 2eB)^2 - 4(\omega^2 - k_z^2)^2(p_{n'}k_z - \omega\varepsilon'_{k2})^2}{k_z^4(\omega^2 - k_z^2 - 2eB)^2 - 4(\omega^2 - k_z^2)^2(p_{n'}k_z + \omega\varepsilon'_{k2})^2} \right| \right. \right. \\
&\quad \left. \left. + \ln \left| \frac{4k_z^4\varepsilon_{n'}^{04} - [p_{n'}k_z(\omega^2 - k_z^2 + 2eB) - 2\varepsilon'_{k2}\varepsilon_F(\omega^2 - k_z^2)]^2}{4k_z^4\varepsilon_{n'}^{04} - [p_{n'}k_z(\omega^2 - k_z^2 + 2eB) + 2\varepsilon'_{k2}\varepsilon_F(\omega^2 - k_z^2)]^2} \right| \right) \right] \Big|_{n' \geq 1}, \\
B &= \left[2(\omega^2 - k_z^2) \ln \left(\frac{\varepsilon_F + p_{n'}}{\varepsilon_F - p_{n'}} \right) + \frac{[\omega^2 - k_z^2 - 2(2n' + 1)eB]k_z}{2\varepsilon'_{k1}} \left(-\ln \left| \frac{k_z^4(\omega^2 - k_z^2 - 2eB)^2 - 4(\omega^2 - k_z^2)^2(p_{n'}k_z - \omega\varepsilon'_{k1})^2}{k_z^4(\omega^2 - k_z^2 - 2eB)^2 - 4(\omega^2 - k_z^2)^2(p_{n'}k_z + \omega\varepsilon'_{k1})^2} \right| \right. \right. \\
&\quad \left. \left. + \ln \left| \frac{4k_z^4\varepsilon_{n'}^{04} - [p_{n'}k_z(\omega^2 - k_z^2 - 2eB) - 2\varepsilon'_{k1}\varepsilon_F(\omega^2 - k_z^2)]^2}{4k_z^4\varepsilon_{n'}^{04} - [p_{n'}k_z(\omega^2 - k_z^2 - 2eB) + 2\varepsilon'_{k1}\varepsilon_F(\omega^2 - k_z^2)]^2} \right| \right) \right] \Big|_{n' \geq 0}, \\
\text{Im } \alpha^{11}|_{\text{LC}} &= -\text{Im } i\alpha^{12}|_{\text{LC}} = \frac{e^3 B}{16\pi} \left(\left| \frac{\omega^2 - k_z^2 - 2(2n + 1)eB}{\omega^2 - k_z^2} \right| \left| \frac{k_z}{\varepsilon_{k1}} I_A \right|_{n \geq 0} + \left| \frac{\omega^2 - k_z^2 - 2(2n' - 1)eB}{\omega^2 - k_z^2} \right| \left| \frac{k_z}{\varepsilon'_{k2}} I_D \right|_{n' \geq 1} \right), \\
\text{Im } \alpha^{11}|_{\text{RC}} &= \text{Im } i\alpha^{12}|_{\text{RC}} = \frac{e^3 B}{16\pi} \left(\left| \frac{\omega^2 - k_z^2 - 2(2n - 1)eB}{\omega^2 - k_z^2} \right| \left| \frac{k_z}{\varepsilon_{k2}} I_C \right|_{n \geq 1} + \left| \frac{\omega^2 - k_z^2 - 2(2n' + 1)eB}{\omega^2 - k_z^2} \right| \left| \frac{k_z}{\varepsilon'_{k1}} I_B \right|_{n' \geq 0} \right), \quad (7)
\end{aligned}$$

where the subscripts LC and RC refer to the left and right circular polarized components, respectively. The nonzero $I_0, I_{A \rightarrow D}$ are given by

$$I_0 = \begin{cases} +2, & k_z < 2p_n, \sqrt{4\varepsilon_n^{02} + k_z^2} < \omega < \varepsilon_F + \sqrt{\varepsilon_F^2 - 2p_n k_z + k_z^2}, \\ +1, & \varepsilon_F + \sqrt{\varepsilon_F^2 - 2p_n k_z + k_z^2} < \omega < \varepsilon_F + \sqrt{\varepsilon_F^2 + 2p_n k_z + k_z^2}, \\ -1, & |\sqrt{\varepsilon_F^2 - 2p_n k_z + k_z^2} - \varepsilon_F| < \omega < \sqrt{\varepsilon_F^2 + 2p_n k_z + k_z^2} - \varepsilon_F, \end{cases} \quad (8)$$

$$I_A = \begin{cases} +2, & k_z < p_n(1 + \varepsilon_{n+1}^0/\varepsilon_n^0), \quad \sqrt{(\varepsilon_n^0 + \varepsilon_{n+1}^0)^2 + k_z^2} < \omega < \varepsilon_F + \sqrt{\varepsilon_F^2 - 2p_n k_z + k_z^2 + 2eB}, \\ +1, & \varepsilon_F + \sqrt{\varepsilon_F^2 - 2p_n k_z + k_z^2 + 2eB} < \omega < \varepsilon_F + \sqrt{\varepsilon_F^2 + 2p_n k_z + k_z^2 + 2eB}, \\ +1, & \text{region 4,} \end{cases}$$

$$I_D = -1, \quad \text{regions } 8', 9',$$

$$I_C = \begin{cases} +2, & k_z < p_n(1 + \varepsilon_{n-1}^0/\varepsilon_n^0), \quad \sqrt{(\varepsilon_n^0 + \varepsilon_{n-1}^0)^2 + k_z^2} < \omega < \varepsilon_F + \sqrt{\varepsilon_F^2 - 2p_n k_z + k_z^2 - 2eB}, \\ +1, & \varepsilon_F + \sqrt{\varepsilon_F^2 - 2p_n k_z + k_z^2 - 2eB} < \omega < \varepsilon_F + \sqrt{\varepsilon_F^2 + 2p_n k_z + k_z^2 - 2eB}, \\ +1, & \text{regions 7, 8,} \\ +1, & \text{region 6,} \\ +2, & \text{region 5,} \end{cases} \quad (9)$$

$$I_B = \begin{cases} -1, & \text{regions } 3', 4', \\ -1, & \text{region } 2', \\ -2, & \text{region } 1', \end{cases} \quad (10)$$

and where $\varepsilon_k = k_z \beta_0 / \omega$, $\varepsilon_{k1} = k_z \beta_1 / \omega$, $\varepsilon_{k2} = k_z \beta_2 / \omega$, $\varepsilon'_{k1} = k_z \beta'_1 / \omega$, $\varepsilon'_{k2} = k_z \beta'_2 / \omega$. The different numbered regions in the gyromagnetic absorption regimes for $\text{Im } \alpha^{11}$ and $\text{Im } i\alpha^{12}$ are as follows:

$$\text{region 1, } 0 < k_z < p_n \left(\frac{\varepsilon_{n+1}^0}{\varepsilon_n^0} - 1 \right), \quad \sqrt{\varepsilon_F^2 + 2p_n k_z + k_z^2 + 2eB} - \varepsilon_F < \omega < \sqrt{(\varepsilon_n^0 - \varepsilon_{n+1}^0)^2 + k_z^2},$$

$$\text{region 2, } 0 < k_z < \frac{eB}{\varepsilon_F - p_n}, \quad [|\sqrt{\varepsilon_F^2 - 2p_n k_z + k_z^2 + 2eB} - \varepsilon_F|, k_z]_{\text{max}} < \omega < \sqrt{\varepsilon_F^2 + 2p_n k_z + k_z^2 + 2eB} - \varepsilon_F,$$

$$\begin{aligned}
&\text{region 3, } k_z > \frac{eB}{\varepsilon_F + p_n}, \quad |\sqrt{\varepsilon_F^2 - 2p_n k_z + k_z^2 + 2eB} - \varepsilon_F| < \omega < [k_z, \sqrt{\varepsilon_F^2 + 2p_n k_z + k_z^2 + 2eB} - \varepsilon_F]_{\min}, \\
&\text{region 4, } p_n^2 > 2eB, p_n - \sqrt{p_n^2 - 2eB} < k_z < p_n + \sqrt{p_n^2 - 2eB}, \quad 0 < \omega < |\sqrt{\varepsilon_F^2 - 2p_n k_z + k_z^2 + 2eB} - \varepsilon_F|, \\
&\text{region 5, } 0 < k_z < p_n \left(1 - \frac{\varepsilon_{n-1}^0}{\varepsilon_n^0}\right), \quad |\sqrt{\varepsilon_F^2 - 2p_n k_z + k_z^2 - 2eB} - \varepsilon_F| < \omega < \sqrt{(\varepsilon_n^0 - \varepsilon_{n-1}^0)^2 + k_z^2}, \\
&\text{region 6, } 0 < k_z < \frac{eB}{\varepsilon_F - p_n}, \quad [|\sqrt{\varepsilon_F^2 + 2p_n k_z + k_z^2 - 2eB} - \varepsilon_F|, k_z]_{\max} < \omega < |\sqrt{\varepsilon_F^2 - 2p_n k_z + k_z^2 - 2eB} - \varepsilon_F|, \\
&\text{region 7, } \frac{eB}{\varepsilon_F + p_n} < k_z < \frac{\sqrt{2eB\varepsilon_F}}{\varepsilon_n^0}, \\
&\quad |\sqrt{\varepsilon_F^2 + 2p_n k_z + k_z^2 - 2eB} - \varepsilon_F| < \omega < [k_z, |\sqrt{\varepsilon_F^2 - 2p_n k_z + k_z^2 - 2eB} - \varepsilon_F|]_{\min}, \\
&\text{region 8, } \sqrt{p_n^2 + 2eB} - p_n < k_z < \sqrt{p_n^2 + 2eB} + p_n, \\
&\quad 0 < \omega < [|\sqrt{\varepsilon_F^2 - 2p_n k_z + k_z^2 - 2eB} - \varepsilon_F|, |\sqrt{\varepsilon_F^2 + 2p_n k_z + k_z^2 - 2eB} - \varepsilon_F|]_{\min}, \\
&\text{region 9, } k_z > \frac{\sqrt{2eB\varepsilon_F}}{\varepsilon_n^0}, \quad |\sqrt{\varepsilon_F^2 - 2p_n k_z + k_z^2 - 2eB} - \varepsilon_F| < \omega < |\sqrt{\varepsilon_F^2 + 2p_n k_z + k_z^2 - 2eB} - \varepsilon_F|, \tag{11}
\end{aligned}$$

with the primed regions being as the unprimed with n replaced by n' .

These different regions for the imaginary parts in the ω - k_z plane are presented in Fig. 1 for the parameters $p_F=2.2$ m, $B=B_{cr}$ for which n_{\max} is 2. These parameters were chosen to give an n_{\max} not too large so that the number of solutions to the dispersion relations in the dissipative regions was a manageable number for a cleaner description of the main trends. The different regions in the PC and GA dissipative regimes for α^{33} are depicted in Fig. 1(a) for an n value of 1. The solid and dotted lines are the $\omega=k_z$ and $\omega=\omega_{PC|n=1}$ lines, respectively. The equations to the lines labelled ω_{P1} and ω_{P2} in the PC regime are $(\varepsilon_F^2 + 2p_n k_z + k_z^2)^{1/2} + \varepsilon_F$ and $(\varepsilon_F^2 - 2p_n k_z + k_z^2)^{1/2} + \varepsilon_F$, respectively, with ω_{P2} being equal to the PC threshold at $k_z=2p_n$. The equations to the lines labelled ω_{G1} and ω_{G2} in the GA regime are $(\varepsilon_F^2 + 2p_n k_z + k_z^2)^{1/2} - \varepsilon_F$ and $|(\varepsilon_F^2 - 2p_n k_z + k_z^2)^{1/2} - \varepsilon_F|$, respectively. The value of I_0 is +2 between the lines $\omega_{PC}=(4\varepsilon_n^{02} + k_z^2)^{1/2}$ and ω_{P2} for k_z satisfying $k_z < 2p_n$; +1 between the lines ω_{P2} and ω_{P1} ; and, -1 between the lines ω_{G2} and ω_{G1} . The different regions for both α^{11} and $i\alpha^{12}$ in the PC regime are similar to those in Fig. 1(a) with the equations to the lines ω_{P1} and ω_{P2} being $(\varepsilon_F^2 \pm 2p_n k_z + k_z^2 + 2eB)^{1/2} + \varepsilon_F$, respectively, arising from the $n \geq 0$ term (viz. A) and $(\varepsilon_F^2 \pm 2p_n k_z + k_z^2 - 2eB)^{1/2} + \varepsilon_F$, respectively, arising from the $n \geq 1$ term (viz. C). The k_z values where $(\varepsilon_F^2 - 2p_n k_z + k_z^2 \pm 2eB)^{1/2} + \varepsilon_F$ are equal to the PC thresholds are $p_n(1 + \varepsilon_{n+1}^0/\varepsilon_n^0)$. The values of $I_{A,C}$ are +2 between the lines $\omega_{PC}=[(\varepsilon_n^0 + \varepsilon_{n\pm 1}^0)^2 + k_z^2]^{1/2}$ and ω_{P2} for $k_z < p_n(1 + \varepsilon_{n\pm 1}^0/\varepsilon_n^0)$,

and +1 between the lines ω_{P2} and ω_{P1} for arbitrary k_z . The numbered regions in (11) in the GA dissipative regime of α^{11} and $i\alpha^{12}$ are drawn for two values of η , namely $\eta=1$ in Fig. 1(b) satisfying $p_\eta^2 > 2eB$ and $\eta=2$ in Fig. 1(d) satisfying $p_\eta^2 < 2eB$, where $\eta=n, n'$ for Im A, Im B, and polarizations e_\pm^μ , respectively. For Im D, Im C with polarizations e_\pm^μ , a single value of $\eta(=n', n)$ of 1 was chosen in Fig. 1(c) as there was no significant difference in the forms of the regions for different η values.

In the regime $\omega_{GA} < \omega < \omega_{PC}$, the components α^{33} , α^{11} , $i\alpha^{12}$ are real. The forms of the response tensors in this dissipation-free (DF) zone can be obtained from their forms above the PC threshold or below the GA edge by the method of analytic continuation. Specifically treating n' as a dummy variable and setting equal to n , the $\varepsilon_k, \varepsilon_{k1}, \varepsilon_{k2}$ become $i\varepsilon_k'', i\varepsilon_{k1}'', i\varepsilon_{k2}''$ with

$$\begin{aligned}
\varepsilon_k'' &= \frac{k_z}{2} \sqrt{\frac{4\varepsilon_n^{02}}{\omega^2 - k_z^2} - 1}, \\
\varepsilon_{k1}'' &= \frac{k_z}{2} \sqrt{\frac{4\varepsilon_n^{02}}{\omega^2 - k_z^2} - \frac{(\omega^2 - k_z^2 - 2eB)^2}{(\omega^2 - k_z^2)^2}}, \\
\varepsilon_{k2}'' &= \frac{k_z}{2} \sqrt{\frac{4\varepsilon_n^{02}}{\omega^2 - k_z^2} - \frac{(\omega^2 - k_z^2 + 2eB)^2}{(\omega^2 - k_z^2)^2}},
\end{aligned}$$

so that, in the DF zone ($\omega_{GA|n} < \omega < \omega_{PC|n}$), the linear response tensors are as follows:

$$\begin{aligned}
\alpha^{33}|_n &= -\frac{e^3 B \omega^2 k_z}{\pi^2 (\omega^2 - k_z^2)^2} \frac{\varepsilon_n^{02} a_n}{\varepsilon_k''} \left[\arctan(1/y) - \begin{cases} \arctan(1/x), & x > 0 \\ \pi + \arctan(1/x), & x < 0 \end{cases} \right], \\
\alpha^{11}|_n &= \frac{e^3 B}{8\pi^2 (\omega^2 - k_z^2)} \left\{ 2(\omega^2 - k_z^2) \ln \left(\frac{\varepsilon_F + p_n}{\varepsilon_F - p_n} \right) - \frac{[\omega^2 - k_z^2 - 2(2n+1)eB]k_z}{\varepsilon_{k1}''} \left[\begin{cases} \arctan(1/y_1), & y_1 > 0 \\ \pi + \arctan(1/y_1), & y_1 < 0 \end{cases} \right. \right. \\
&\quad \left. \left. - \begin{cases} \arctan(1/x_1), & x_1 > 0 \\ \pi + \arctan(1/x_1), & x_1 < 0 \end{cases} \right] \right\}, \\
&+ \frac{e^3 B}{8\pi^2 (\omega^2 - k_z^2)} \left\{ 2(\omega^2 - k_z^2) \ln \left(\frac{\varepsilon_F + p_n}{\varepsilon_F - p_n} \right) - \frac{[\omega^2 - k_z^2 - 2(2n-1)eB]k_z}{\varepsilon_{k2}''} \left[\arctan(1/y_2) - \begin{cases} \arctan(1/x_2), & x_2 > 0 \\ \pi + \arctan(1/x_2), & x_2 < 0 \end{cases} \right] \right\} \Big|_{n>0}, \\
i\alpha^{12}|_n &= \frac{e^3 B}{8\pi^2 (\omega^2 - k_z^2)} \frac{[\omega^2 - k_z^2 - 2(2n+1)eB]k_z}{\varepsilon_{k1}''} \left[\begin{cases} \arctan(1/y_3), & y_3 > 0 \\ \pi + \arctan(1/y_3), & y_3 < 0 \end{cases} - \begin{cases} \arctan(1/x_3), & x_3 > 0 \\ \pi + \arctan(1/x_3), & x_3 < 0 \end{cases} \right] \\
&- \frac{e^3 B}{8\pi^2 (\omega^2 - k_z^2)} \frac{[\omega^2 - k_z^2 - 2(2n-1)eB]k_z}{\varepsilon_{k2}''} \left[\arctan(1/y_4) - \begin{cases} \arctan(1/x_4), & x_4 > 0 \\ \pi + \arctan(1/x_4), & x_4 < 0 \end{cases} \right] \Big|_{n>0}, \quad (12)
\end{aligned}$$

where

$$\begin{aligned}
x &= \frac{k_z [2\varepsilon_n^{02} k_z - p_n (\omega^2 - k_z^2)]}{2\varepsilon_k'' \varepsilon_F (\omega^2 - k_z^2)}, \\
y &= \frac{k_z [2\varepsilon_n^{02} k_z + p_n (\omega^2 - k_z^2)]}{2\varepsilon_k'' \varepsilon_F (\omega^2 - k_z^2)} > 0, \\
x_1 &= \frac{k_z [2k_z \varepsilon_n^{02} - p_n (\omega^2 - k_z^2 - 2eB)]}{2\varepsilon_{k1}'' \varepsilon_F (\omega^2 - k_z^2)}, \\
y_1 &= \frac{k_z [2k_z \varepsilon_n^{02} + p_n (\omega^2 - k_z^2 - 2eB)]}{2\varepsilon_{k1}'' \varepsilon_F (\omega^2 - k_z^2)}, \\
x_2 &= \frac{k_z [2k_z \varepsilon_n^{02} - p_n (\omega^2 - k_z^2 + 2eB)]}{2\varepsilon_{k2}'' \varepsilon_F (\omega^2 - k_z^2)}, \\
y_2 &= \frac{k_z [2k_z \varepsilon_n^{02} + p_n (\omega^2 - k_z^2 + 2eB)]}{2\varepsilon_{k2}'' \varepsilon_F (\omega^2 - k_z^2)} > 0, \\
x_3 &= \frac{k_z [k_z (\omega^2 - k_z^2 - 2eB) - 2p_n (\omega^2 - k_z^2)]}{2\omega \varepsilon_{k1}'' (\omega^2 - k_z^2)}, \\
y_3 &= \frac{k_z [k_z (\omega^2 - k_z^2 - 2eB) + 2p_n (\omega^2 - k_z^2)]}{2\omega \varepsilon_{k1}'' (\omega^2 - k_z^2)}, \\
x_4 &= \frac{k_z [k_z (\omega^2 - k_z^2 + 2eB) - 2p_n (\omega^2 - k_z^2)]}{2\omega \varepsilon_{k2}'' (\omega^2 - k_z^2)}, \\
y_4 &= \frac{k_z [k_z (\omega^2 - k_z^2 + 2eB) + 2p_n (\omega^2 - k_z^2)]}{2\omega \varepsilon_{k2}'' (\omega^2 - k_z^2)} > 0. \quad (13)
\end{aligned}$$

With $\omega_{PC}|_n < \omega_{PC}|_{n+1}$ for all response tensors and $\omega_{PC}|_{n'} < \omega_{PC}|_{n'+1}$, $\omega_{GA}|_n > \omega_{GA}|_{n+1}$, $\omega_{GA}|_{n'} > \omega_{GA}|_{n'+1}$ for

$\alpha^{11}, i\alpha^{12}$, some of the $\alpha^{\mu\nu}|_n$ terms in the sum (6) may be in the dissipative regime while others may be in the nondissipative regime depending upon the value of ω for given k_z, B . For example, consider the linear response tensor α^{33} and an ω satisfying $(4\varepsilon_0^{02} + k_z^2)^{1/2} < \omega < (4\varepsilon_1^{02} + k_z^2)^{1/2}$ for which the $n=0$ term is of a natural logarithm form as in (7) whereas the other terms ($n>0$) are of an arctan form as in (12). Note that for an ω in the GA region of α^{33} , for which the gyromagnetic edge is equal to k_z , all the terms are of a natural logarithm form as given in (7).

III. DISPERSION RELATIONS

The homogeneous wave equation for an electromagnetic field in a medium is of the form

$$\Lambda^{\mu\nu}(k) A_\nu(k) = 0,$$

$$\Lambda^{\mu\nu}(k) = k^2 g^{\mu\nu} - k^\mu k^\nu + 4\pi \alpha^{\mu\nu(H)}(k), \quad (14)$$

where $A^\mu(k)$ is the 4-potential. The source terms have been neglected and consequently only the Hermitian (H) part of the linear response tensor is retained, viz.

$$\alpha^{\mu\nu(H)}(k) = \frac{1}{2} [\alpha^{\mu\nu}(k) + \alpha^{*\nu\mu}(k)].$$

Constructing the tensors $\lambda^{\mu\nu}(k)$, whose elements are the cofactors of $\Lambda^{\mu\nu}(k)$, and using the gauge invariance and charge continuity conditions, $k_\nu \Lambda^{\mu\nu}(k) = 0$ and $k_\mu \Lambda^{\mu\nu}(k) = 0$, one has $\lambda^{\mu\nu}(k) = k^\mu k^\nu \lambda(k)$, where $\lambda(k)$ is an invariant. The dispersion equation becomes

$$\lambda(k) = 0, \quad (15)$$

any particular solution, $\omega = \omega_M(k)$, of which is the dispersion relation for a wave mode M [14]. Explicit evaluation of $\lambda(k)$ gives the following dispersion relations:

$$\begin{aligned}\omega^2 - 4\pi\alpha^{33(H)} &= \omega^2 - 4\pi \text{Re}(\alpha^{33} + \alpha_{\text{vac}}^{33}) \\ &= \omega^2 - 4\pi \text{Re}(\alpha^{33})_{\text{total}} = 0,\end{aligned}$$

$$\begin{aligned}k^2 - 4\pi(\alpha^{11(H)} + i\alpha^{12(H)}) &= \omega^2 - k_z^2 - 4\pi \text{Re}(\alpha^{11} + i\alpha^{12})_{\text{total}} \\ &= \omega^2 - k_z^2 - 4\pi \text{Re}(\alpha_+) = 0,\end{aligned}$$

$$\begin{aligned}k^2 - 4\pi(\alpha^{11(H)} - i\alpha^{12(H)}) &= \omega^2 - k_z^2 - 4\pi \text{Re}(\alpha^{11} - i\alpha^{12})_{\text{total}} \\ &= \omega^2 - k_z^2 - 4\pi \text{Re}(\alpha_-) = 0,\end{aligned}\quad (16)$$

the first of which is defined as the longitudinal (L) mode with polarization tensor $e_L^\mu = (0, 0, 0, 1)$ and the latter two as the transverse modes (\pm) with polarization tensors $e_\pm^\mu = 2^{-1/2}(0, 1, \pm i, 0)$, respectively. These dispersion relations represent the dominant non- k_\perp dependent solutions in the oblique angle limit (θ small) of $\lambda(k)=0$, the lowest order in k_\perp being k_\perp^2 . Although the vacuum contributions to the Her-

mitian parts of the linear response tensors in the dispersion relations are small compared to the particle contributions over much of ω - k_z space, the singularities that arise at each PC threshold cancel out the analogous singularities in the particle contributions. Inclusion of the vacuum contributions to the Hermitian parts of the linear response tensors is therefore imperative. The same is true for the imaginary vacuum contributions that occur above the PC thresholds.

The electron contributions to the imaginary parts of α^{33} are given in (7). The vacuum contributions to the imaginary parts of α^{33} are also as in (7) but with an I_0 given by -2 for frequencies satisfying $\omega > (4\varepsilon_n^{02} + k_z^2)^{1/2}$. The sum of these contributions then gives the total contribution to the imaginary parts of α^{33} as

$$\text{Im}(\alpha^{33})_{\text{total}} = \frac{e^3 B}{2\pi} \frac{\varepsilon_n^{02} \omega^2 k_z a_n}{\varepsilon_k (\omega^2 - k_z^2)^2} I_0, \quad (17)$$

with

$$I_0 = \begin{cases} 0, & k_z < 2p_n, \quad \sqrt{4\varepsilon_n^{02} + k_z^2} < \omega < \varepsilon_F + \sqrt{\varepsilon_F^2 - 2p_n k_z + k_z^2}, & \text{two cancel,} \\ -2, & k_z > 2p_n, \quad \sqrt{4\varepsilon_n^{02} + k_z^2} < \omega < \varepsilon_F + \sqrt{\varepsilon_F^2 - 2p_n k_z + k_z^2}, & \text{full vacuum,} \\ -1, & \varepsilon_F + \sqrt{\varepsilon_F^2 - 2p_n k_z + k_z^2} < \omega < \varepsilon_F + \sqrt{\varepsilon_F^2 + 2p_n k_z + k_z^2}, & \text{half-vacuum,} \\ -2, & \omega > \varepsilon_F + \sqrt{\varepsilon_F^2 + 2p_n k_z + k_z^2}, & \text{full vacuum,} \\ -1, & |\sqrt{\varepsilon_F^2 - 2p_n k_z + k_z^2} - \varepsilon_F| < \omega < \sqrt{\varepsilon_F^2 + 2p_n k_z + k_z^2} - \varepsilon_F, & \text{full electron.} \end{cases} \quad (18)$$

The imaginary parts of $\alpha^{11} + i\alpha^{12}$ due to the electrons are given by the sum of $\text{Im } \alpha^{11}$ and $\text{Im } i\alpha^{12}$ in (7), viz. $2 \text{Im } \alpha^{11}$, polarization e_+^μ (I_C and I_B only) and those of $\alpha^{11} - i\alpha^{12}$ by the difference of $\text{Im } \alpha^{11}$ and $\text{Im } i\alpha^{12}$ in (7), viz. $2 \text{Im } \alpha^{11}$, polarization e_-^μ (I_A and I_D only). The imaginary parts of $\alpha^{11} \pm i\alpha^{12}$ due to the vacuum are also given by the sum and difference of α^{11} and $i\alpha^{12}$ as given in (7) but with only I_C and I_A being nonzero and having the value -2 for $\omega > [(\varepsilon_n^0 + \varepsilon_{n-1}^0)^2 + k_z^2]^{1/2}$ and $\omega > [(\varepsilon_n^0 + \varepsilon_{n+1}^0)^2 + k_z^2]^{1/2}$, respectively. The sums of the electron and vacuum contributions give the total contributions to the imaginary parts of $\alpha^{11} \pm i\alpha^{12}$ which are as follows:

$$\text{Im}(\alpha_+)|_{\text{RC}} = \frac{e^3 B}{8\pi} \left\{ \left| \frac{\omega^2 - k_z^2 - 2(2n-1)eB}{\omega^2 - k_z^2} \right| \left| \frac{k_z}{\varepsilon_{k2}} I_C \right|_{n \geq 1} + \left| \frac{\omega^2 - k_z^2 - 2(2n'+1)eB}{\omega^2 - k_z^2} \right| \left| \frac{k_z}{\varepsilon'_{k1}} I_B \right|_{n' \geq 0} \right\}, \quad (19)$$

with

$$I_C = \begin{cases} 0, & k_z < p_n(1 + \varepsilon_{n-1}^0/\varepsilon_n^0), \quad \sqrt{(\varepsilon_n^0 + \varepsilon_{n-1}^0)^2 + k_z^2} < \omega < \varepsilon_F + \sqrt{\varepsilon_F^2 - 2p_n k_z + k_z^2} - 2eB, & \text{two cancel,} \\ -2, & k_z > p_n(1 + \varepsilon_{n-1}^0/\varepsilon_n^0), \quad \sqrt{(\varepsilon_n^0 + \varepsilon_{n-1}^0)^2 + k_z^2} < \omega < \varepsilon_F + \sqrt{\varepsilon_F^2 - 2p_n k_z + k_z^2} - 2eB, & \text{full vacuum,} \\ -1, & \varepsilon_F + \sqrt{\varepsilon_F^2 - 2p_n k_z + k_z^2} - 2eB < \omega < \varepsilon_F + \sqrt{\varepsilon_F^2 + 2p_n k_z + k_z^2} - 2eB, & \text{half-vacuum,} \\ -2, & \omega > \varepsilon_F + \sqrt{\varepsilon_F^2 + 2p_n k_z + k_z^2} - 2eB, & \text{full vacuum,} \\ +1, & \text{regions 7, 8,} & \text{full electron} \\ +1, & \text{region 6,} & \text{full electron,} \\ +2, & \text{region 5,} & \text{full electron,} \end{cases}$$

$$I_B = \begin{cases} -1, & \text{regions 3', 4',} & \text{full electron} \\ -1, & \text{region 2',} & \text{full electron} \\ -2, & \text{region 1',} & \text{full electron,} \end{cases} \quad (20)$$

and

$$\text{Im}(\alpha_-)|_{\text{LC}} = \frac{e^3 B}{8\pi} \left(\left| \frac{\omega^2 - k_z^2 - 2(2n+1)eB}{\omega^2 - k_z^2} \right| \left| \frac{k_z}{\varepsilon_{k1}} I_A \right|_{n \geq 0} + \left| \frac{\omega^2 - k_z^2 - 2(2n'-1)eB}{\omega^2 - k_z^2} \right| \left| \frac{k_z}{\varepsilon'_{k2}} I_D \right|_{n' \geq 1} \right), \quad (21)$$

with

$$I_A = \begin{cases} 0, & k_z < p_n(1 + \varepsilon_{n+1}^0/\varepsilon_n^0), \sqrt{(\varepsilon_n^0 + \varepsilon_{n+1}^0)^2 + k_z^2} < \omega < \varepsilon_F + \sqrt{\varepsilon_F^2 - 2p_n k_z + k_z^2 + 2eB}, & \text{two cancel,} \\ -2, & k_z > p_n(1 + \varepsilon_{n+1}^0/\varepsilon_n^0), \sqrt{(\varepsilon_n^0 + \varepsilon_{n+1}^0)^2 + k_z^2} < \omega < \varepsilon_F + \sqrt{\varepsilon_F^2 - 2p_n k_z + k_z^2 + 2eB}, & \text{full vacuum,} \\ -1, & \varepsilon_F + \sqrt{\varepsilon_F^2 - 2p_n k_z + k_z^2 + 2eB} < \omega < \varepsilon_F + \sqrt{\varepsilon_F^2 + 2p_n k_z + k_z^2 + 2eB}, & \text{half-vacuum,} \\ -2, & \omega > \varepsilon_F + \sqrt{\varepsilon_F^2 + 2p_n k_z + k_z^2 + 2eB}, & \text{full vacuum,} \\ +1, & \text{region 4,} & \text{full electron,} \end{cases}$$

$$I_D = -1, \quad \text{regions } 8', 9', \quad \text{full electron.} \quad (22)$$

In deriving the longitudinal and transverse modes below, the vacuum contributions to the Hermitian parts of the linear response tensors are taken from Bakshi, Cover, and Kalman [15].

A. Longitudinal modes

There are a number of possible modes satisfying the dispersion relation

$$\omega^2 - 4\pi \text{Re}(\alpha^{33})_{\text{total}} = 0, \quad (23)$$

namely, the gyromagnetic absorption and pair creation modes below the GA edge at $\omega = k_z$ and above the PC thresh-

old at $\omega = (4\varepsilon_0^{02} + k_z^2)^{1/2}$, respectively, originating when the numerator or denominator of the argument of the natural logarithm in $\text{Re } \alpha^{33}|_n$ of (7) passes through zero, and a mode ω_L beginning in the nondissipative regime $[k_z < \omega < (4\varepsilon_0^{02} + k_z^2)^{1/2}]$ at low k_z then cutting the light line and extending into the gyromagnetic regime at higher k_z similar in nature to the longitudinal mode of an unmagnetized degenerate electron gas. Each of these modes are discussed below.

1. Gyromagnetic absorption modes

Rewriting $\text{Re } \alpha^{33}|_n$ as

$$\begin{aligned} \text{Re } \alpha^{33}|_n = & -\frac{e^3 B}{2\pi^2} \frac{\varepsilon_n^{02} \omega^2 k_z a_n}{\varepsilon_k(k_z^2 - \omega^2)^2} \times \left(\ln \left| \frac{k_z[2\varepsilon_n^{02} k_z + p_n(k_z^2 - \omega^2)] + 2\varepsilon_k \varepsilon_F(k_z^2 - \omega^2)}{k_z[2\varepsilon_n^{02} k_z + p_n(k_z^2 - \omega^2)] - 2\varepsilon_k \varepsilon_F(k_z^2 - \omega^2)} \right| \right. \\ & \left. - \ln \left| \frac{k_z[2\varepsilon_n^{02} k_z - p_n(k_z^2 - \omega^2)] + 2\varepsilon_k \varepsilon_F(k_z^2 - \omega^2)}{k_z[2\varepsilon_n^{02} k_z - p_n(k_z^2 - \omega^2)] - 2\varepsilon_k \varepsilon_F(k_z^2 - \omega^2)} \right| \right), \end{aligned} \quad (24)$$

and the dispersion relation as $1 - 4\pi \text{Re}(\alpha^{33})_{\text{total}}/\omega^2 = 0$, then the denominators of the arguments of the first and second natural logarithm terms in (24) are zero at frequencies $|\varepsilon_F - (\varepsilon_F^2 - 2p_n k_z + k_z^2)^{1/2}|$ and $(\varepsilon_F^2 + 2p_n k_z + k_z^2)^{1/2} - \varepsilon_F$ such that $\text{Re } \alpha^{33} \rightarrow \mp \infty$, respectively. If the left-hand side (LHS) of the dispersion relation is negative as one approaches $|\varepsilon_F - (\varepsilon_F^2 - 2p_n k_z + k_z^2)^{1/2}|$ from below, then a mode occurs on either side of $\omega = |\varepsilon_F - (\varepsilon_F^2 - 2p_n k_z + k_z^2)^{1/2}|$ as $4\pi \text{Re } \alpha^{33}/\omega^2 \rightarrow -\infty$. If, however, the LHS of the dispersion relation is positive as one approaches $(\varepsilon_F^2 + 2p_n k_z + k_z^2)^{1/2} - \varepsilon_F$ from below, then a mode occurs on either side of $\omega = (\varepsilon_F^2 + 2p_n k_z + k_z^2)^{1/2} - \varepsilon_F$ as $4\pi \text{Re } \alpha^{33}/\omega^2 \rightarrow +\infty$. This behavior is shown in Fig. 2(a) where $1 - 4\pi \text{Re}(\alpha^{33})_{\text{total}}/\omega^2$ is plotted as a function of ω ($0 < \omega < k_z$) for the parameters $B = B_{cr}$, $p_F = 2.2$ m, and $k_z = 0.1$ m ($n_{\text{max}} = 2$). There are three peak-trough arrangements, the peaks ($\text{Re } \alpha^{33} \rightarrow -\infty$) occurring at $|\varepsilon_F - (\varepsilon_F^2 - 2p_n k_z + k_z^2)^{1/2}|$ and the troughs ($\text{Re } \alpha^{33} \rightarrow +\infty$) at $(\varepsilon_F^2 + 2p_n k_z + k_z^2)^{1/2} - \varepsilon_F$, with the arrangement lowest in frequency corresponding to $n = n_{\text{max}}$ and highest to $n = 0$. Just before each

arrangement begins, $1 - 4\pi \text{Re}(\alpha^{33})_{\text{total}}/\omega^2$ is positive (true for arbitrary B , p_F , and k_z) resulting in two modes for each n , $1 \leq n \leq n_{\text{max}}$, at frequencies

$$\omega = \sqrt{\varepsilon_F^2 + 2p_n k_z + k_z^2} - \varepsilon_F \pm \delta_{\pm}, \quad \delta_- < \delta_+,$$

as $1 - 4\pi \text{Re}(\alpha^{33})_{\text{total}}/\omega^2$ tends to $-\infty$ and passes through zero twice, either side of $(\varepsilon_F^2 + 2p_n k_z + k_z^2)^{1/2} - \varepsilon_F$. When $n = 0$, a single mode occurs just below $(\varepsilon_F^2 + 2p_F k_z + k_z^2)^{1/2} - \varepsilon_F$, viz.

$$\omega = \sqrt{\varepsilon_F^2 + 2p_F k_z + k_z^2} - \varepsilon_F - \delta_- \approx \sqrt{\varepsilon_F^2 + 2p_F k_z + k_z^2} - \varepsilon_F,$$

as $1 - 4\pi \text{Re}(\alpha^{33})_{\text{total}}/\omega^2$ approaches $-\infty$. Eventually it passes through zero and forms the mode ω_L discussed below. The line ω_{G1} in Fig. 1(a) is the $n = 1$ value of $(\varepsilon_F^2 + 2p_n k_z + k_z^2)^{1/2} - \varepsilon_F$ either side of which a doublet mode occurs. As one steps through frequency searching for the sign change in $1 - 4\pi \text{Re}(\alpha^{33})_{\text{total}}/\omega^2$, the separation between the two components of the doublet mode is wide enough to be easily discernible [step size $\Delta\omega \approx 10^{-3}$ for the parameters in Fig. 2(a)].

2. Mode ω_L near the light line

At low k_z , this mode begins above the light line, cuts the light line at a k_z value of k_0 say, and then at larger k_z becomes the line $(\varepsilon_F^2 + 2p_F k_z + k_z^2)^{1/2} - \varepsilon_F + \delta_+$, namely the higher frequency $n=0$ doublet of the logarithmic singularity of the GA mode. The value of k_0 can be estimated via the $\omega^2 - k_z^2 \rightarrow 0$ limit of the plasma part of (23), viz.

$$k_0^2 \simeq \frac{4e^3 B \varepsilon_F}{\pi} \sum_{n=0}^{n_{\max}} \frac{p_n a_n}{\varepsilon_n^{02}}. \quad (25)$$

In Fig. 2(b), the different longitudinal modes, namely the gyromagnetic absorption modes (solid short-dashed lines a, b, c for $n=0, 1, 2$, respectively), ω_L (solid black line indecipherable from line a) and the pair modes (lines A, B, C discussed below), are presented for the parameters $p_F = 2.2m$ and $B = B_{cr}$. The grey dotted lines are the corresponding PC thresholds.

3. Pair modes

Rewriting $\text{Re } \alpha^{33}|_n$ as

$$\begin{aligned} \text{Re } \alpha^{33}|_n &= \frac{e^3 B}{2\pi^2} \frac{\varepsilon_n^{02} \omega^2 k_z a_n}{\varepsilon_k(\omega^2 - k_z^2)^2} \\ &\times \left(\ln \left| \frac{k_z[2\varepsilon_n^{02} k_z - p_n(\omega^2 - k_z^2)] + 2\varepsilon_k \varepsilon_F(\omega^2 - k_z^2)}{k_z[2\varepsilon_n^{02} k_z - p_n(\omega^2 - k_z^2)] - 2\varepsilon_k \varepsilon_F(\omega^2 - k_z^2)} \right| \right. \\ &\left. - \ln \left| \frac{k_z[2\varepsilon_n^{02} k_z + p_n(\omega^2 - k_z^2)] + 2\varepsilon_k \varepsilon_F(\omega^2 - k_z^2)}{k_z[2\varepsilon_n^{02} k_z + p_n(\omega^2 - k_z^2)] - 2\varepsilon_k \varepsilon_F(\omega^2 - k_z^2)} \right| \right) \end{aligned} \quad (26)$$

for $\omega > \omega_{PC|n}$, and the dispersion relation as $1 - 4\pi \text{Re}(\alpha^{33})_{\text{total}}/\omega^2 = 0$, then for $k_z < 2p_n$ the numerator and denominator of the arguments of the first and second natural logarithms in (26) are zero at frequencies $\varepsilon_F + (\varepsilon_F^2 - 2p_n k_z + k_z^2)^{1/2}$ and $\varepsilon_F + (\varepsilon_F^2 + 2p_n k_z + k_z^2)^{1/2}$ such that $\text{Re } \alpha^{33} \rightarrow \mp \infty$, respectively. When $k_z > 2p_n$, the denominators of the argument of the first and second natural logarithms are zero at $\varepsilon_F + (\varepsilon_F^2 - 2p_n k_z + k_z^2)^{1/2}$ and $\varepsilon_F + (\varepsilon_F^2 + 2p_n k_z + k_z^2)^{1/2}$, respectively, resulting in $\text{Re } \alpha^{33} \rightarrow +\infty$ in both cases. If the LHS of the dispersion relation is positive as one approaches $\varepsilon_F + (\varepsilon_F^2 - 2p_n k_z + k_z^2)^{1/2}$ from below then a mode only occurs when $k_z > 2p_n$ on the approach and departure of $\varepsilon_F + (\varepsilon_F^2 - 2p_n k_z + k_z^2)^{1/2}$ as $\text{Re } \alpha^{33}/\omega^2 \rightarrow +\infty$. If, on the other hand, the LHS of the dispersion relation is negative as one approaches either $\varepsilon_F + (\varepsilon_F^2 + 2p_n k_z + k_z^2)^{1/2}$ (for all k_z) or $\varepsilon_F + (\varepsilon_F^2 - 2p_n k_z + k_z^2)^{1/2}$ (for $k_z < 2p_n$) from below, then modes only occur either side of these two frequencies as $\text{Re } \alpha^{33}/\omega^2 \rightarrow -\infty$.

For $k_z < 2p_n$, one has $1 - 4\pi \text{Re}(\alpha^{33})_{\text{total}}/\omega^2 > 0$ just above the PC thresholds and no modes arise. For $k_z > 2p_n$, $1 - 4\pi \text{Re}(\alpha^{33})_{\text{total}}/\omega^2$ is positive and pair modes occur either side of $\varepsilon_F + (\varepsilon_F^2 - 2p_n k_z + k_z^2)^{1/2}$, viz.

$$\omega = \varepsilon_F + \sqrt{\varepsilon_F^2 - 2p_n k_z + k_z^2} \pm \delta \simeq \varepsilon_F + \sqrt{\varepsilon_F^2 - 2p k_z + k_z^2}.$$

These pair modes are presented in Fig. 2(b) for the parameters $p_F = 2.2m$ and $B = B_{cr}$, viz. the black dashed-double-dotted lines A, B, C are the $n=0, 1, 2$ pair modes $\varepsilon_F + (\varepsilon_F^2$

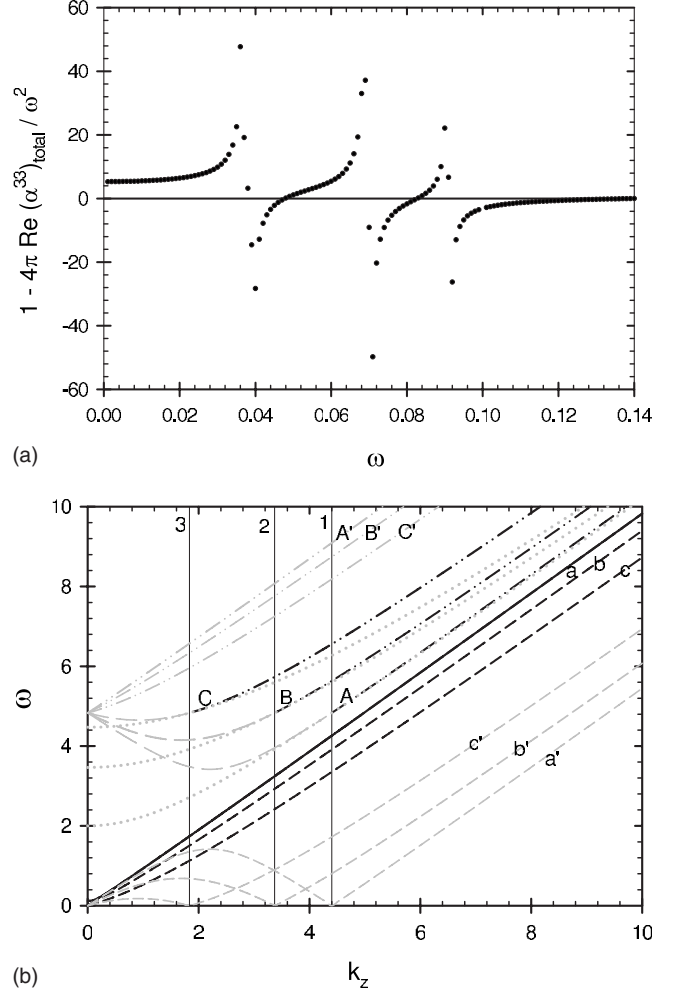


FIG. 2. (a): The left-hand side of the longitudinal dispersion relation, $1 - 4\pi \text{Re}(\alpha^{33})_{\text{total}}/\omega^2 = 0$, is plotted as a function of ω , $0 < \omega < k_z$, for the parameters $p_F = 2.2m$, $B = B_{cr}$, and $k_z = 0.1m$. Peaks and troughs occur at the logarithmic singularities when one has $\omega = |(\varepsilon_F^2 \mp 2p_n k_z + k_z^2)^{1/2} - \varepsilon_F|$, respectively. (b) The different longitudinal modes for the parameters $p_F = 2.2m$ and $B = B_{cr}$. The different lines are discussed in the text.

$-2p_n k_z + k_z^2)^{1/2}$, respectively, that lie above wave numbers $2p_n$ (viz. to the right of lines 1, 2, 3). Their continuation into regimes where they are no longer modes are drawn as the grey long-dashed lines. The lines A', B', C' are the $n=0, 1, 2$ components of $(\varepsilon_F^2 + 2p_n k_z + k_z^2)^{1/2} + \varepsilon_F$, respectively, drawn as grey long-dashed lines. By including these lines, the extent of the dissipation experienced by each of the pair modes becomes apparent. For example, all pair mode doublets lie entirely within dissipative regimes; the amount of dissipation is greatest when the modes are closest to their PC thresholds; and, each pair mode with $n > 0$ has the additional imaginary contributions from the pair modes of lower n values.

B. Transverse modes

The transverse modes satisfying the dispersion relation

$$\omega^2 - k_z^2 - 4\pi \text{Re}(\alpha_{\pm}) = 0 \quad (27)$$

comprise the pair modes above the PC thresholds analogous to the longitudinal case; modes ω_{\pm} below the $[(\epsilon_1^0 - \epsilon_0^0)^2 + k_z^2]^{1/2}$ gyromagnetic edge similar to the transverse mode for an unmagnetized, degenerate electron gas; a mode just above each gyromagnetic absorption edge for the (α_+) component; and, the more complicated gyromagnetic absorption modes for $0 < \omega < \omega_{GA}|_{n_{\max}}$.

1. Modes below and just above the gyromagnetic absorption edges

There are transverse modes, denoted by ω_{\pm} , with polarization e_{\pm}^{μ} of an analogous nature to the unmagnetized transverse mode, that occur below the GA edge and asymptote to the light line from above for large k_z . For a given k_z , they occur when the dispersion relation (27) is satisfied, the LHS of which increases smoothly with ω from below zero to above zero. The LHS of the dispersion relation is negative or positive depending upon whether the frequency ω satisfies $0 < \omega < \omega_{\pm}$ or $\omega > \omega_{\pm}$, respectively. Superimposed on this smoothly varying function are the peaks and troughs of the modes made up of the GA modes and modes just above the GA edges. Both ω_{\pm} modes are situated at frequencies satisfying $\omega < \omega_{GA}|_{n_{\max}}$.

A mode is possible with polarization e_{+}^{μ} at each n , $1 \leq n \leq n_{\max}$ or n' , $0 \leq n' \leq n_{\max}$ should $\omega^2 - k_z^2 - 4\pi \text{Re}(\alpha_+)$ be ini-

tially negative or positive before approaching $\pm\infty$ at the gyromagnetic edges at $[(\epsilon_{\eta}^0 - \epsilon_{\eta-1}^0)^2 + k_z^2]^{1/2}$, $\eta = n, n'$ from above for $k_z < p_n(1 - \epsilon_{n-1}^0/\epsilon_n^0)$ or $k_z < p_{n'}(\epsilon_{n'+1}^0/\epsilon_{n'}^0 - 1)$, respectively. For $k_z < p_n(1 - \epsilon_{n-1}^0/\epsilon_n^0)$, the two $\omega^2 - k_z^2 - \text{Re}(\alpha_+)$ values, one at each n , $1 \leq n \leq n_{\max}$ and the other at each n' , $0 \leq n' \leq n_{\max} - 1$, sum to zero, the value of $p_n(1 - \epsilon_{n-1}^0/\epsilon_n^0)$ being less than $k_z < p_{n'}(\epsilon_{n'+1}^0/\epsilon_{n'}^0 - 1)$. For $p_{n'+1}(1 - \epsilon_{n'}^0/\epsilon_{n'+1}^0) < k_z < p_{n'}(\epsilon_{n'+1}^0/\epsilon_{n'}^0 - 1)$, $0 \leq n' \leq n_{\max} - 1$ and $k_z < p_{n'}(\epsilon_{n'+1}^0/\epsilon_{n'}^0 - 1)$, $n' = n_{\max}$, however, modes occur ($G0, G1, \dots$, say) above their respective GA edges, $[(\epsilon_{n'+1}^0 - \epsilon_n^0)^2 + k_z^2]^{1/2}$, $\omega^2 - k_z^2 - 4\pi \text{Re}(\alpha_+)$ being initially positive as $\omega > \omega_{GA}(>\omega_+)$. Each of these modes, over a restricted range of k_z , contributes two solutions to the dispersion relation, the first (lower in frequency) essentially at the GA edge as the LHS of the dispersion relation changes from finite, positive to $-\infty$, and the second ($G0, G1, \dots$) as the LHS of the dispersion relation returns to a finite, positive value. This second solution can be a considerable distance away from the edge [e.g., $B = B_{cr}$, $p_F = 2.2m$, $k_z = 0$, $n' = 2$, first peak at $(\epsilon_3^0 - \epsilon_2^0) = 0.4096m$, second peak at $(\epsilon_3^0 - \epsilon_2^0) + \delta = 0.4230m$, $\delta = 0.0134m$]. No analogous modes exist for the transverse component $\text{Re}(\alpha_-)$.

The GA modes occur when the arguments of the numerators or denominators of the natural logarithms in $4\pi \text{Re}(\alpha^{11} \pm i\alpha^{12})|_{\eta=n',n}$ viz.

$$4\pi \text{Re}(\alpha^{11} + i\alpha^{12})|_{\eta=n',n} = [T1(n') - P1(n')]_{n' \geq 0} + [T2(n) + P2(n)]_{n \geq 1},$$

$$4\pi \text{Re}(\alpha^{11} - i\alpha^{12})|_{\eta=n',n} = [T1(n) + P1(n)]_{n \geq 0} + [T2(n') - P2(n')]_{n' \geq 1},$$

$$\begin{aligned} T1(\eta) &= \frac{e^3 B}{2\pi} \left[2 \ln \left(\frac{\epsilon_F + p_{\eta}}{\epsilon_F - p_{\eta}} \right) \right. \\ &\quad \left. + \frac{[\omega^2 - k_z^2 - 2(2\eta + 1)eB]}{\sqrt{(\omega^2 - k_z^2 - 2eB)^2 - 4\epsilon_{\eta}^{02}(\omega^2 - k_z^2)}} \ln \left| \frac{4k_z^2 \epsilon_{\eta}^{04} - [p_{\eta}(\omega^2 - k_z^2 - 2eB) - \sqrt{(\omega^2 - k_z^2 - 2eB)^2 - 4\epsilon_{\eta}^{02}(\omega^2 - k_z^2)} \epsilon_F]^2}{4k_z^2 \epsilon_{\eta}^{04} - [p_{\eta}(\omega^2 - k_z^2 - 2eB) + \sqrt{(\omega^2 - k_z^2 - 2eB)^2 - 4\epsilon_{\eta}^{02}(\omega^2 - k_z^2)} \epsilon_F]^2} \right| \right], \\ P1(\eta) &= \frac{e^3 B}{2\pi} \frac{[\omega^2 - k_z^2 - 2(2\eta + 1)eB]}{\sqrt{(\omega^2 - k_z^2 - 2eB)^2 - 4\epsilon_{\eta}^{02}(\omega^2 - k_z^2)}} \\ &\quad \times \ln \left| \frac{k_z^2(\omega^2 - k_z^2 - 2eB)^2 - [2p_{\eta}(\omega^2 - k_z^2) - \omega \sqrt{(\omega^2 - k_z^2 - 2eB)^2 - 4\epsilon_{\eta}^{02}(\omega^2 - k_z^2)}]^2}{k_z^2(\omega^2 - k_z^2 - 2eB)^2 - [2p_{\eta}(\omega^2 - k_z^2) + \omega \sqrt{(\omega^2 - k_z^2 - 2eB)^2 - 4\epsilon_{\eta}^{02}(\omega^2 - k_z^2)}]^2} \right|, \\ T2(\eta) &= \frac{e^3 B}{2\pi^2} \left[2 \ln \left(\frac{\epsilon_F + p_{\eta}}{\epsilon_F - p_{\eta}} \right) \right. \\ &\quad \left. + \frac{[\omega^2 - k_z^2 - 2(2\eta - 1)eB]}{\sqrt{(\omega^2 - k_z^2 + 2eB)^2 - 4\epsilon_{\eta}^{02}(\omega^2 - k_z^2)}} \ln \left| \frac{4k_z^2 \epsilon_{\eta}^{04} - [p_{\eta}(\omega^2 - k_z^2 + 2eB) - \sqrt{(\omega^2 - k_z^2 + 2eB)^2 - 4\epsilon_{\eta}^{02}(\omega^2 - k_z^2)} \epsilon_F]^2}{4k_z^2 \epsilon_{\eta}^{04} - [p_{\eta}(\omega^2 - k_z^2 + 2eB) + \sqrt{(\omega^2 - k_z^2 + 2eB)^2 - 4\epsilon_{\eta}^{02}(\omega^2 - k_z^2)} \epsilon_F]^2} \right| \right], \end{aligned}$$

$$P2(\eta) = \frac{e^3 B}{2\pi^2} \frac{(\omega^2 - k_z^2 - 2(2\eta - 1)eB)}{\sqrt{(\omega^2 - k_z^2 + 2eB)^2 - 4\epsilon_\eta^2(\omega^2 - k_z^2)}} \times \ln \left| \frac{k_z^2(\omega^2 - k_z^2 + 2eB)^2 - [2p_\eta(\omega^2 - k_z^2) - \omega\sqrt{(\omega^2 - k_z^2 + 2eB)^2 - 4\epsilon_\eta^2(\omega^2 - k_z^2)}]^2}{k_z^2(\omega^2 - k_z^2 + 2eB)^2 - [2p_\eta(\omega^2 - k_z^2) + \omega\sqrt{(\omega^2 - k_z^2 + 2eB)^2 - 4\epsilon_\eta^2(\omega^2 - k_z^2)}]^2} \right|, \quad (28)$$

are zero, whereby the right-hand side (RHS) of (28) tends to $+\infty$ or $-\infty$ over a small range of frequencies. Should these logarithmic singularities cause the LHS of the dispersion relation to pass through zero (either side of the singularity), then these doublet modes are defined as the GA modes. The four possible GA modes for each polarization lie on either side of $|(\epsilon_F^2 \pm 2p_\eta k_z + k_z^2 + 2eB)^{1/2} - \epsilon_F|$, $0 \leq \eta \leq n_{\max}$ with $\eta = n, n'$ (polarization e_\pm^μ) and $|(\epsilon_F^2 \pm 2p_\eta k_z + k_z^2 - 2eB)^{1/2} - \epsilon_F|$, $1 \leq \eta \leq n_{\max}$ with $\eta = n, n'$ (polarization e_\pm^μ). The frequencies of the possible modes, polarization e_\pm^μ , in relation to ω_\pm determine which of these occur.

For the transverse component $\text{Re}(\alpha_-)$, the GA modes, with possible values of n, n' in the ranges $0 \leq n \leq n_{\max}$, $1 \leq n' \leq n_{\max}$ and polarization e_\pm^μ , are

$$\omega|_n \approx |\sqrt{\epsilon_F^2 - 2p_n k_z + k_z^2 + 2eB} - \epsilon_F|, \quad p_n^2 > 2eB, \quad p_n - \sqrt{p_n^2 - 2eB} < k_z < p_n + \sqrt{p_n^2 - 2eB}, \quad (29)$$

and

$$\omega|_{n'} \approx |\sqrt{\epsilon_F^2 - 2p_{n'} k_z + k_z^2 - 2eB} - \epsilon_F|, \quad k_z > p_{n'} + \sqrt{p_{n'}^2 + 2eB}, \quad (30)$$

for ω satisfying $0 < \omega < k_z$. These GA doublet modes are

situated below the light line ($\omega < \omega_-$) and are drawn as single lines for convenience in Fig. 3(a) for the parameters $B = B_{cr}$ and $p_F = 2.2m$ ($n_{\max} = 2$). The modes are drawn in black, their continuations into regimes where they are no longer modes are drawn in grey. The ω_- mode is drawn as the solid black line, the $n=0$ and 1 dispersion relations satisfying (29) (labeled C and D) are drawn as the dotted lines, and the $n' = 1$ and 2 dispersion relations satisfying (30) (labeled A and B) are drawn as the dashed lines. In descending frequency, the grey dashed-dotted lines are the $n=0, 1, 2$ components of $(\epsilon_F^2 + 2p_n k_z + k_z^2 + 2eB)^{1/2} - \epsilon_F$ and the grey solid lines are the $n'=1$ and 2 components of $|(\epsilon_F^2 + 2p_{n'} k_z + k_z^2 - 2eB)^{1/2} - \epsilon_F|$. By including these components and comparing Fig. 3(a) with Figs. 1(b) and 1(c), the dissipative regions 4 and 8', 9', respectively, are apparent. For example, consider the lower frequency modes of the doublets labeled A, C and B, D. The former are in nondissipative regimes and the latter are partially in both nondissipative and dissipative regimes. The higher frequency modes of all these doublets, however, are in dissipative regions.

For the transverse component $\text{Re}(\alpha_+)$, the GA modes with possible values of n, n' in the ranges $1 \leq n \leq n_{\max}$, $0 \leq n' \leq n_{\max}$ and polarization e_\pm^μ are

$$\omega|_{n'} \approx |\sqrt{\epsilon_F^2 - 2p_{n'} k_z + k_z^2 + 2eB} - \epsilon_F| \quad \begin{cases} p_{n'}^2 < 2eB, & k_z > eB/(\epsilon_F + p_{n'}), \\ p_{n'}^2 > 2eB, & eB/(\epsilon_F + p_{n'}) < k_z < p_{n'} - \sqrt{p_{n'}^2 - 2eB}, \quad k_z > p_{n'} + \sqrt{p_{n'}^2 - 2eB}, \end{cases} \quad (31)$$

$$\omega|_n \approx |\sqrt{\epsilon_F^2 - 2p_n k_z + k_z^2 - 2eB} - \epsilon_F|, \quad eB/(\epsilon_F - p_n) < k_z < p_n + \sqrt{p_n^2 + 2eB}, \quad (32)$$

with $0 < \omega < [k_z, \omega_+]_{\min}$,

$$\omega|_{n'} \approx |\sqrt{\epsilon_F^2 + 2p_{n'} k_z + k_z^2 + 2eB} - \epsilon_F|, \quad k_z > eB/(\epsilon_F - p_{n'}), \quad (33)$$

$$\omega|_n \approx |\sqrt{\epsilon_F^2 + 2p_n k_z + k_z^2 - 2eB} - \epsilon_F|, \quad eB/(\epsilon_F + p_n) < k_z < \sqrt{p_n^2 + 2eB} - p_n, \quad (34)$$

for $k_z > \omega_+$, $\omega_+ < \omega < k_z$ or

$$\omega|_{n'} \approx \begin{cases} |\sqrt{\epsilon_F^2 - 2p_{n'} k_z + k_z^2 + 2eB} - \epsilon_F|, & 0 < k_z < eB/(\epsilon_F + p_{n'}), \\ |\sqrt{\epsilon_F^2 + 2p_{n'} k_z + k_z^2 + 2eB} - \epsilon_F|, & 0 < k_z < p_{n'}(\epsilon_{n'+1}^0/\epsilon_{n'}^0 - 1), \end{cases} \quad (35)$$

$$\omega|_n \approx |\sqrt{\epsilon_F^2 - 2p_n k_z + k_z^2 - 2eB} - \epsilon_F|, \quad p_n(1 - \epsilon_{n-1}^0/\epsilon_n^0) < k_z < eB/(\epsilon_F - p_n), \quad (36)$$

for $k_z < \omega_+$, $k_z < \omega < \omega_+$, and

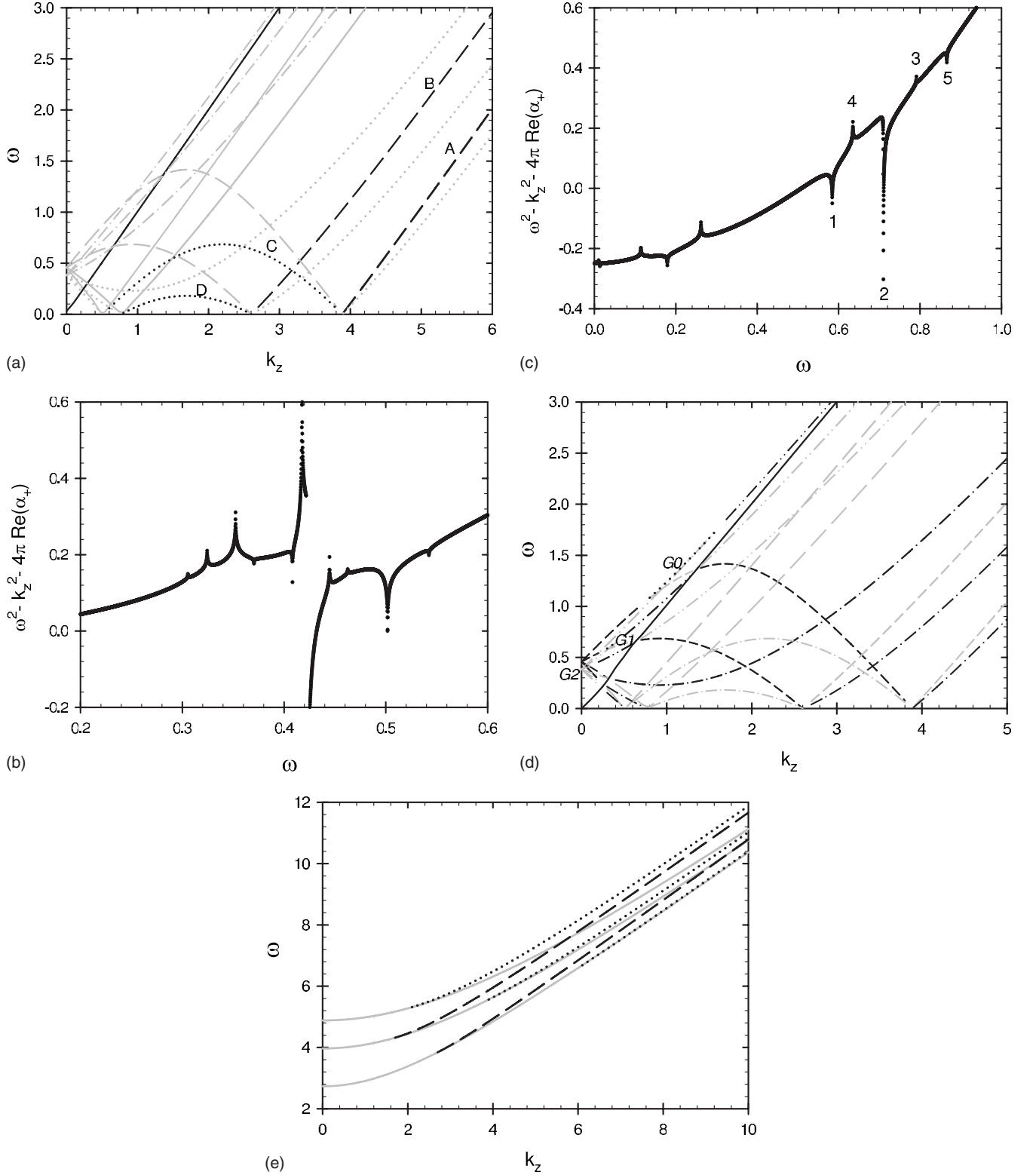


FIG. 3. (a): The gyromagnetic absorption modes are plotted as a function of k_z for the transverse component $\text{Re}(\alpha_-)$ with polarization e_-^μ , for the parameters $p_F = 2.2m$ and $B = B_{cr}$. The solid line represents the mode ω_- , the dotted lines labeled C and D are the $n=0$ and $n=1$ values, respectively, of ω_n in (29). The long-dashed lines labeled A and B are the $n'=1$ and $n'=2$ values, respectively, of (30). (b) The left-hand side of the transverse dispersion relation $\omega^2 - k_z^2 - 4\pi \text{Re}(\alpha_+) = 0$ is plotted as a function of ω ($0 < \omega < \omega_{GA}$) for the parameters $p_F = 2.2m$, $B = B_{cr}$, $\Delta\omega = 10^{-4}m$, and $k_z = 0.1m$. (c) As for (b) but for $k_z = 0.5m$. (d) The gyromagnetic absorption modes are plotted as a function of k_z for the transverse component $\text{Re}(\alpha_+)$ with polarization e_+^μ , for the parameters $p_F = 2.2m$ and $B = B_{cr}$. The different lines are defined in the text. (e) Transverse pair modes above the pair creation thresholds for the parameters $p_F = 2.2m$ and $B = B_{cr}$. See the text for a description of the different lines.

$$\omega|_{n'} \approx \sqrt{\varepsilon_F^2 + 2p_{n'}k_z + k_z^2 + 2eB} - \varepsilon_F, \quad p_{n'}(\varepsilon_{n'+1}^0/\varepsilon_{n'}^0 - 1) < k_z < eB/(\varepsilon_F - p_{n'}), \quad (37)$$

$$\omega|_n \approx \begin{cases} |\sqrt{\varepsilon_F^2 + 2p_nk_z + k_z^2 - 2eB} - \varepsilon_F|, & 0 < k_z < eB/(\varepsilon_F + p_n), \\ |\sqrt{\varepsilon_F^2 - 2p_nk_z + k_z^2 - 2eB} - \varepsilon_F|, & 0 < k_z < p_n(1 - \varepsilon_{n-1}^0/\varepsilon_n^0), \end{cases} \quad (38)$$

with $[k_z, \omega_+]_{\max} < \omega < \omega_{GA}$. In Figs. 3(b) and 3(c), $\omega^2 - k_z^2 - 4\pi \text{Re}(\alpha_+)$ is plotted as a function of ω ($0 < \omega < \omega_{GA}$) for the parameters $B=B_{cr}$, $p_F=2.2m$, $\Delta\omega=10^{-4}m$, and $k_z=0.1m$ and $0.5m$, respectively. Whether $|(\varepsilon_F^2 \pm 2p_{n'}k_z + k_z^2 + 2eB)^{1/2} - \varepsilon_F|$, $|(\varepsilon_F^2 \pm 2p_nk_z + k_z^2 - 2eB)^{1/2} - \varepsilon_F|$, $\eta=n'n$, respectively, are modes or not is determined by their location in ω - k_z space as dictated by (31)–(38).

For $k_z=0.1m$, $\omega^2 - k_z^2 - 4\pi \text{Re}(\alpha_+)$ is positive as one approaches each logarithmic singularity, viz. $\omega > \omega_+$. The first three peaks in Fig. 3(b) correspond to the $n'=0, 1, 2$ components of (31) and do not form solutions to the dispersion relation. The next two troughs do form GA modes and are the $n=1, 2$ components of the first case in (38). The next three peaks do not form GA modes as they belong to the $n'=2, 1, 0$ components of (37), a k_z value of $0.1m$ being below the minimum k_z of $p_{n'}(\varepsilon_{n'+1}^0/\varepsilon_{n'}^0 - 1)$ required to form a mode. The distinct trough at $k_z \sim 0.42m$, between the $n'=2$ and $n'=1$ components of (37), which along with the $n'=0$ component do not form modes, corresponds to the mode G2 just above the GA edge at $[(\varepsilon_{n'+1}^0 - \varepsilon_{n'}^0)^2 + k_z^2]^{1/2}$, $n'=2$ [the $n'=0, 1$ components (troughs) being canceled out at this low k_z value by the corresponding $n=1, 2$ components (peaks)]. Finally the last two troughs form modes and correspond to the second case in (38). These modes are all doublets.

For $k_z=0.5m$, ω_+ has the value $0.5088m$. The first three peaks in Fig. 3(c) occur below ω_+ and hence form the GA modes given in (31), the k_z of $0.5m$ being greater than $eB/(\varepsilon_F + p_{n'})$ but less than $p_{n'} - (p_{n'}^2 - 2eB)^{1/2}$ for $n'=0, 1, 2$. Interspersed within these three peaks are the two troughs at $\omega = |(\varepsilon_F^2 + 2p_{n'}k_z + k_z^2 - 2eB)^{1/2} - \varepsilon_F|$, $n=1, 2$, which do not form GA modes as they do not satisfy the $\omega_+ < \omega < \omega_{GA}$ condition in the first case of (38). The next peaks and troughs occur when $\omega > \omega_+$. The two troughs and peak marked 1, 2, and 3, respectively, correspond to the $n'=2, 1, 0$ values of $|(\varepsilon_F^2 + 2p_{n'}k_z + k_z^2 + 2eB)^{1/2} - \varepsilon_F|$ of (37). Although the condition $\omega_+ < \omega < \omega_{GA}$ is satisfied, the k_z condition $p_{n'}(\varepsilon_{n'+1}^0/\varepsilon_{n'}^0 - 1) < k_z < eB/(\varepsilon_F - p_{n'})$ is only satisfied for $n'=2, 1$ (the two troughs), these forming GA modes. The peak and trough marked 4 and 5, respectively, correspond to the $n=2$ and $n=1$ values of $|(\varepsilon_F^2 - 2p_nk_z + k_z^2 - 2eB)^{1/2} - \varepsilon_F|$, the second case of (38), the k_z restriction only being satisfied for the $n=1$ case which consequently forms a GA mode. The doublet nature of the modes is easily discernible for the frequency step of $10^{-4}m$ chosen in Figs. 3(b) and 3(c), the separation between the two modes of the doublet being the order of a few step sizes.

In Fig. 3(d), the GA modes are drawn in black for the transverse mode α_+ as a function of k_z . As ω_+ and k_z are indiscernible on the scale of Fig. 3(d), only the modes arising from Eqs. (31), (32), (37), and (38) are considered. The

short-dashed lines are the $n=1, 2$ components of $|(\varepsilon_F^2 - 2p_nk_z + k_z^2 - 2eB)^{1/2} - \varepsilon_F|$ in (32) and the second equation in (38); the dashed-dotted lines are the $n'=0, 1, 2$ components of $|(\varepsilon_F^2 - 2p_{n'}k_z + k_z^2 + 2eB)^{1/2} - \varepsilon_F|$ of (31); the long-dashed lines are the $n=1, 2$ components of $|(\varepsilon_F^2 + 2p_nk_z + k_z^2 - 2eB)^{1/2} - \varepsilon_F|$ of the first equation in (38); and, the dashed-double-dotted lines are the $n'=0, 1, 2$ components of $|(\varepsilon_F^2 + 2p_{n'}k_z + k_z^2 + 2eB)^{1/2} - \varepsilon_F|$ of (37). The dotted lines labeled G0, G1, and G2 are the truncated $n'=0, 1$ and the entire $n'=2$ [$0 < k_z < p_{n'}(\varepsilon_{n'+1}^0/\varepsilon_{n'}^0 - 1)$] components, respectively, of the mode just above the GA edges (for convenience drawn as the single mode at the appropriate GA edge). The line labeled G2 on the scale used in Fig. 3(d) is only discernible as two dots near $\omega \sim 0.4m$. The continuation of (31), (32), (37), and (38) into regimes where they are no longer modes are drawn in grey. Comparing Fig. 3(d) with Fig. 1(c) and Figs. 1(b) and 1(d), the dissipative regions 7, 8 and 3', 4', respectively, are apparent. Determination of the ω_+ mode was made difficult at times by the presence of the resonant modes, a problem exacerbated for B and p_F parameters generating large n_{\max} values. The GA modes for the $\text{Re}(\alpha_-)$ component lie below the light line and consequently caused no problems when determining the ω_- mode.

2. Pair modes above the pair creation thresholds

The next set of transverse modes are the pair modes above the PC thresholds arising when the numerator or denominator of the arguments of the natural logarithms in $4\pi \text{Re}(\alpha^{11} \pm i\alpha^{12})$ as given in (28) tend to zero such that $\omega^2 - k_z^2 - 4\pi \text{Re}(\alpha_{\pm})$ passes through zero.

With $4\pi \text{Re}(\alpha^{11} \pm i\alpha^{12})$ as in (28) and $\omega^2 - k_z^2 - 4\pi \text{Re}(\alpha_{\pm})$ positive above the PC thresholds, pair modes arise from the n -dependent terms when $4\pi \text{Re}(\alpha^{11} \pm i\alpha^{12})$ tends to $+\infty$. For the transverse components $\text{Re}(\alpha^{11} \pm i\alpha^{12})$, this corresponds to

$$\begin{aligned} \omega &= \varepsilon_F + \sqrt{\varepsilon_F^2 - 2p_nk_z + k_z^2 \mp 2eB} \pm \delta \\ &\approx \varepsilon_F + \sqrt{\varepsilon_F^2 - 2p_nk_z + k_z^2 \mp 2eB}, \end{aligned} \quad (39)$$

with polarization e_{\pm}^{μ} for $k_z > p_n(1 + \varepsilon_{n+1}^0/\varepsilon_n^0)$ and n between 1 or 0 and n_{\max} , respectively. These pair modes are depicted in Fig. 3(e) for the parameters $B=B_{cr}$ and $p_F=2.2m$. In this figure, the dotted lines in ascending frequency are the $n=0, 1$, and 2 components of the pair mode $\varepsilon_F + (\varepsilon_F^2 - 2p_nk_z + k_z^2 + 2eB)^{1/2}$ for the transverse mode $\text{Re}(\alpha_-)$ with polarization e_{-}^{μ} ; the dashed lines in ascending frequency are the $n=1$ and 2 components of the pair mode $\varepsilon_F + (\varepsilon_F^2 - 2p_nk_z + k_z^2 - 2eB)^{1/2}$ for the transverse mode $\text{Re}(\alpha_+)$ with polarization e_{+}^{μ} ; and, the solid grey lines are the respective PC thresholds drawn in for

reference. The pair modes given by the doublet (39) are drawn as single dispersion curves.

IV. RESULTS AND DISCUSSION

Before summarizing the main features of the dispersive properties of a parallel-propagating, magnetic degenerate electron gas, the results are compared with the unmagnetized case and previous work. In the same manner as the numerator or denominator of the arguments of the natural logarithm terms in $\text{Re } \alpha^{33}$ and $\text{Re}(\alpha^{11} \pm i\alpha^{12})$ for the magnetized case pass through zero, so they do for the unmagnetized case at $\omega = \varepsilon_F + (\varepsilon_F^2 \pm 2p_F|\mathbf{k}| + |\mathbf{k}|^2)^{1/2}$ and $\omega = \varepsilon_F - (\varepsilon_F^2 \pm 2p_F|\mathbf{k}| + |\mathbf{k}|^2)^{1/2}$ [16]. However, unlike the magnetized case where pair and gyromagnetic absorption doublet modes occur for the longitudinal and two transverse modes, the coefficient in front of the natural logarithm in the unmagnetized case is zero such that

$$\lim_{x \rightarrow 0} x \ln x \rightarrow 0$$

and no such analogous modes exist.

The unmagnetized transverse mode, ω_T say, and the magnetized transverse modes ω_{\pm} behave similarly, beginning above the light line (except for the ω_+ mode which begins below the light line, crossing it at some low k_z) and then asymptoting to it from above at large $|\mathbf{k}|$, k_z , respectively. In the magnetized case however, these modes are in the dissipative regime below the gyromagnetic absorption edge whereas in the unmagnetized case the mode occurs in the dissipation-free zone, $|\mathbf{k}| < \omega_T < (4m^2 + |\mathbf{k}|^2)^{1/2}$. The longitudinal mode for the unmagnetized case, $\omega_L(|\mathbf{k}|)$, forms a tonguelike feature [16], which cuts the light line at some $|\mathbf{k}|$, the upper $\omega_L(0)$ value being above the light line and the lower $\omega_L(0)$ value being below. The longitudinal mode near the light line for a magnetized gas also begins in the dissipation-free zone, cuts the light line at k_0 and becomes the higher frequency $n=0$ component of the gyromagnetic absorption doublet mode.

The polarization matrix element $i\Pi_{12}$ presented in the work by Cover, Kalman, and Bakshi and Pérez Rojas and Shabad is opposite in sign to the $i\Pi_{12}$ [$=i\alpha_{12}/(4\pi)$] presented here, resulting in Π_{\pm} corresponding to their Π_{\mp} ($=\Pi_{11} \mp i\Pi_{12}$). Taking the cold plasma limit of the longitudinal (α^{33}) and the two transverse ($\alpha^{11} \pm i\alpha^{12}$) components in (4), one obtains

$$K_3^3 = 1 - \frac{\omega_p^2}{\omega^2}, \quad K_1^1 \pm iK_2^1 = 1 - \frac{\omega_p^2}{\omega^2} \frac{1}{1 \mp \omega_c/\omega}, \quad (40)$$

for the dielectric response tensors ($K_j^i = \delta_j^i + 4\pi\alpha_j^i/\omega^2$), where ω_p and ω_c are the plasma and cyclotron frequencies, respectively. As $\alpha^{11} \pm i\alpha^{12}$ in this limit correctly reproduces the x and o modes, respectively, one finds that the sign difference in $i\alpha^{12}$ between the authors in [7–9] and that obtained here is due to differences in convention. Taking this into account, the real parts of the response tensors as presented in Eqs. (7) and (12) taken in the limit $k_z=0$ agree with the results of Cover, Kalman, and Bakshi [7]. Further, the pair modes (pair creation collective modes) of Pulsifer and Kalman [8] are reproduced.

In this paper, the real and imaginary parts of the response tensors for a parallel-propagating, magnetized, degenerate electron gas have been presented along with a study of the resultant longitudinal and transverse modes. The modes resulting from a logarithmic singularity, such as the pair modes and the gyromagnetic absorption modes, are doublets since $\lambda(k)$ given by (16) passes through zero twice, namely, on either side of the singularity. One of the modes of the doublets has a $\partial\lambda/\partial\omega$ value which is positive and the other a value which is necessarily negative. Should the mode be in a dissipative regime, then the latter produces a negative energy wave [see (42) below].

In the limit of weak damping, the damping coefficient $\gamma_M(k)$ of the mode M , whereby the energy in the waves varies as $\exp[-\gamma_M(k)t]$, is given by [14]

$$\gamma_M(k) = 2i \frac{R_M(k)}{\omega_M} 4\pi\alpha_M^A(k), \quad (41)$$

with α_M^A related to the anti-Hermitian part of the response tensor, viz. $\alpha_M^A(k) = e_{M\alpha}^* e_{M\beta} \alpha^{A\alpha\beta}(k_M)$, and equal to $i \text{Im}(\alpha^{33})_{\text{total}}|_{\omega_M}$ and $i \text{Im}(\alpha_{\pm})|_{\omega_M}$ for the longitudinal and transverse modes, respectively. The quantity $R_M(k)$ is the ratio of electric to total energy in the waves, viz.

$$[R_M(k)]^{-1} = - \left(\frac{1}{\omega} \frac{\partial \Lambda_M}{\partial \omega} \right)_{\omega_M}, \quad (42)$$

with $\Lambda_M = e_{M\mu}^* e_{M\nu} \Lambda^{H\mu\nu}$ and $\Lambda^{H\mu\nu}$ the Hermitian part of $\Lambda^{\mu\nu} (=k^2 g^{\mu\nu} - k^\mu k^\nu + 4\pi\alpha^{\mu\nu})$ yielding $\Lambda_M = -\lambda_M$ with λ_L and λ_T given by $\omega^2 - 4\pi \text{Re}(\alpha^{33})_{\text{total}}$ and $\omega^2 - k_z^2 - 4\pi \text{Re}(\alpha_{\pm})$, respectively, so that

$$[R_M(k)]^{-1} = \left(\frac{1}{\omega} \frac{\partial \lambda_M}{\partial \omega} \right)_{\omega_M}, \quad (43)$$

and γ_M becomes

$$\gamma_M(k) = - \frac{2}{\omega_M} \left(\frac{1}{\omega} \frac{\partial \lambda_M}{\partial \omega} \right)_{\omega_M}^{-1} 4\pi \text{Im } \alpha_M, \quad (44)$$

where $\text{Im } \alpha_M$ is negative and α_M is equal to $(\alpha^{33})_{\text{total}}|_{\omega_M}$ and $(\alpha_{\pm})|_{\omega_M}$. A mode with a γ_M value greater than zero is a damped wave mode and one with a γ_M value less than zero is a growing wave mode. The amount of damping and/or growth can be insignificant as in the case of the pair modes, the logarithmic singularities being over a small range in frequency. However, for the longitudinal gyromagnetic absorption modes say, it can be significant. The necessary existence of negative energy growing wave modes as part of the growing-damped doublet produced at the mode-forming logarithmic singularities is somewhat puzzling for a degenerate electron gas, as there is no source of free energy. These growing modes, however, invariably have extremely large negative $\partial\lambda/\partial\omega$ values. Either a more complex description than that of weak damping is needed for these doublet modes or the $\partial\lambda/\partial\omega$ values of the growing components are so large as to yield zero growth. If the latter is the case, then the other modes of the GA and pair doublets, with positive $\partial\lambda/\partial\omega$ values, are damped in regions of dissipation. For example,

the pair modes are entirely within dissipative regions whereas the modes just above the gyromagnetic absorption edges for the transverse component α_+ can be entirely in a nondissipative region (e.g., G_0) or partially in both nondissipative and dissipative regions (e.g., G_1, G_2, \dots), the modes being damped when they are in dissipative regions.

The longitudinal mode ω_L is in a nondissipative region. The ω_\pm modes, predominantly lying above the light line, are at times in dissipative regions. Positive $\partial\lambda/\partial\omega|_{\omega_\pm}$ values imply damped wave modes in these regions with γ_M values of considerable strength as ω_\pm are near the light line [and thus $\omega - k_z$ in the denominator of the expression for $\text{Im}(\alpha_\pm)$ is small] and the $\partial\lambda/\partial\omega|_{\omega_\pm}$ values are of the order of m .

ACKNOWLEDGMENTS

The author thanks Don Melrose and Qinghuan Luo for useful comments on the paper.

APPENDIX: VERTEX FUNCTIONS

Since we are summing over the spin states, $[\Pi_{q'q}^{\epsilon'\epsilon}(\mathbf{k})]^{\mu\nu}$ is independent of the choice of spin operator; one may evaluate it by making any explicit choice of spin eigenstates. Choosing coordinate axes

$$\mathbf{B} = (0, 0, B), \quad \mathbf{k} = (k_\perp \cos \psi, k_\perp \sin \psi, k_z), \quad (\text{A1})$$

explicit evaluation gives

$$2\varepsilon'_n \varepsilon_n [\Pi_{n'n}^{\epsilon'\epsilon}(\mathbf{k})]^{00} = (\varepsilon'_n \varepsilon_n + p'_z p_z + \epsilon' \epsilon m^2) [(J_{n'-n}^{n-1})^2 + (J_{n'-n}^n)^2] + 2\epsilon' \epsilon p_n p_n J_{n'-n}^{n-1} J_{n'-n}^n,$$

$$2\varepsilon'_n \varepsilon_n [\Pi_{n'n}^{\epsilon'\epsilon}(\mathbf{k})]^{01} = -\epsilon' \varepsilon_n p_n (J_{n'-n}^{n-1} e^{i\psi} J_{n'-n+1}^{n-1} + J_{n'-n}^n e^{-i\psi} J_{n'-n-1}^n) - \epsilon \varepsilon'_n p_n (J_{n'-n}^n e^{i\psi} J_{n'-n+1}^{n-1} + J_{n'-n}^{n-1} e^{-i\psi} J_{n'-n-1}^n),$$

$$2\varepsilon'_n \varepsilon_n [\Pi_{n'n}^{\epsilon'\epsilon}(\mathbf{k})]^{02} = i\epsilon' \varepsilon_n p_n (J_{n'-n}^{n-1} e^{i\psi} J_{n'-n+1}^{n-1} - J_{n'-n}^n e^{-i\psi} J_{n'-n-1}^n) + i\epsilon \varepsilon'_n p_n (J_{n'-n}^n e^{i\psi} J_{n'-n+1}^{n-1} - J_{n'-n}^{n-1} e^{-i\psi} J_{n'-n-1}^n),$$

$$2\varepsilon'_n \varepsilon_n [\Pi_{n'n}^{\epsilon'\epsilon}(\mathbf{k})]^{03} = (\varepsilon'_n p_z + \varepsilon_n p'_z) [(J_{n'-n}^{n-1})^2 + (J_{n'-n}^n)^2],$$

$$2\varepsilon'_n \varepsilon_n [\Pi_{n'n}^{\epsilon'\epsilon}(\mathbf{k})]^{11} = (\varepsilon'_n \varepsilon_n - p'_z p_z - \epsilon' \epsilon m^2) [(J_{n'-n+1}^{n-1})^2 + (J_{n'-n-1}^n)^2] + 2\epsilon' \epsilon p_n p_n \cos(2\psi) J_{n'-n+1}^{n-1} J_{n'-n-1}^n,$$

$$2\varepsilon'_n \varepsilon_n [\Pi_{n'n}^{\epsilon'\epsilon}(\mathbf{k})]^{22} = (\varepsilon'_n \varepsilon_n - p'_z p_z - \epsilon' \epsilon m^2) [(J_{n'-n+1}^{n-1})^2 + (J_{n'-n-1}^n)^2] - 2\epsilon' \epsilon p_n p_n \cos(2\psi) J_{n'-n+1}^{n-1} J_{n'-n-1}^n,$$

$$2\varepsilon'_n \varepsilon_n [\Pi_{n'n}^{\epsilon'\epsilon}(\mathbf{k})]^{33} = (\varepsilon'_n \varepsilon_n + p'_z p_z - \epsilon' \epsilon m^2) [(J_{n'-n}^{n-1})^2 + (J_{n'-n}^n)^2] - 2\epsilon' \epsilon p_n p_n J_{n'-n}^{n-1} J_{n'-n}^n,$$

$$2\varepsilon'_n \varepsilon_n [\Pi_{n'n}^{\epsilon'\epsilon}(\mathbf{k})]^{12} = -i(\varepsilon'_n \varepsilon_n - p'_z p_z - \epsilon' \epsilon m^2) [(J_{n'-n+1}^{n-1})^2 - (J_{n'-n-1}^n)^2] + 2\epsilon' \epsilon p_n p_n \sin(2\psi) J_{n'-n+1}^{n-1} J_{n'-n-1}^n,$$

$$2\varepsilon'_n \varepsilon_n [\Pi_{n'n}^{\epsilon'\epsilon}(\mathbf{k})]^{13} = -\epsilon' p_n p_z (J_{n'-n}^{n-1} e^{-i\psi} J_{n'-n+1}^{n-1} + J_{n'-n}^n e^{i\psi} J_{n'-n-1}^n) - \epsilon p_n p'_z (J_{n'-n}^n e^{-i\psi} J_{n'-n+1}^{n-1} + J_{n'-n}^{n-1} e^{i\psi} J_{n'-n-1}^n),$$

$$2\varepsilon'_n \varepsilon_n [\Pi_{n'n}^{\epsilon'\epsilon}(\mathbf{k})]^{23} = -i\epsilon' p_n p_z (J_{n'-n}^{n-1} e^{-i\psi} J_{n'-n+1}^{n-1} - J_{n'-n}^n e^{i\psi} J_{n'-n-1}^n) - i\epsilon p_n p'_z (J_{n'-n}^n e^{-i\psi} J_{n'-n+1}^{n-1} - J_{n'-n}^{n-1} e^{i\psi} J_{n'-n-1}^n), \quad (\text{A2})$$

with the J -functions related to generalized Laguerre polynomials,

$$J_\nu^\mu(x) = (-)^{\nu} J_{-\nu}^{\mu+\nu}(x) = \left(\frac{n!}{(n+\nu)!} \right)^{1/2} e^{-x/2} x^{\nu/2} L_n^\nu(x),$$

with argument $x = k_\perp^2 / 2eB$. The tensor is Hermitian, and $[\Pi_{n'n}^{\epsilon'\epsilon}(\mathbf{k})]^{\mu\nu} = [\Pi_{n'n}^{\epsilon'\epsilon}(\mathbf{k})]^{*\nu\mu}$ determines the remaining components in terms of those written in (A2).

- [1] V. N. Tsytovich, Sov. Phys. JETP **13**, 1249 (1961).
- [2] B. Jancovici, Nuovo Cimento **25**, 428 (1963).
- [3] V. Kowalenko, N. E. Frankel, and K. C. Hines, Phys. Rep. **126**, 109 (1985).

- [4] E. Braaten, Phys. Rev. Lett. **66**, 1655 (1991).
- [5] E. Braaten and D. Segel, Phys. Rev. D **48**, 1478 (1993).
- [6] N. Itoh *et al.*, Astrophys. J. **395**, 622 (1992).
- [7] R. A. Cover, G. Kalman, and P. Bakshi, Phys. Rev. D **20**, 3015

- (1979).
- [8] P. Pulsifer and G. Kalman, Phys. Rev. A **45**, 5820 (1992).
- [9] H. Pérez Rojas and A. E. Shabad, Ann. Phys. **138**, 1 (1982).
- [10] E. M. Kantor and M. E. Gusakov, Mon. Not. R. Astron. Soc. **381**, 1702 (2007).
- [11] A. Odrzywolek, Eur. Phys. J. C **52**, 425 (2007).
- [12] D. B. Melrose and A. J. Parle, Aust. J. Phys. **36**, 799 (1983).
- [13] D. B. Melrose and A. J. Parle, Aust. J. Phys. **36**, 755 (1983).
- [14] D. B. Melrose, Aust. J. Phys. **34**, 563 (1981).
- [15] P. Bakshi, R. A. Cover, and G. Kalman, Phys. Rev. D **14**, 2532 (1976).
- [16] J. McOrist, D. B. Melrose, and J. I. Weise, J. Plasma Phys. **74**, 495 (2007).